AN INVESTIGATION OF THE APPLICATION OF THE RAYLEIGH-RITZ METHOD TO THE DEFLECTIONS OF A SMALL ASPECT RATIO SWEPT PLATE OF UNIFORM THICKNESS

Thesis by

Joseph Wolff Wechsler

In Partial Fulfillment of the Requirements

For the Degree of

Aeronautical Engineer

California Institute of Technology

Pasadena, California

1950

ACKNOWLEDGEMENTS

The writer wishes to thank all those whose efforts and interest in this work played an important part in its realization. To Dr. Y. C. Fung he is especially indebted for having originated the method investigated and for continual helpful guidance in carrying out the present study. To Mr. Max Williams who contributed many useful suggestions in the preparation of the manuscript, to Mr. George Hrebec who supervised the experimental program and the preparation of the figures, to Miss Georgette Pauwels and Mrs. Mary-Evelyn Bryden who performed the computations, and to Mrs. Virginia Boughton who typed the manuscript, he also wishes to express his sincere gratitude.

ABSTRACT

An investigation was initiated to examine the possibility of improving the rate of convergence of a series solution for the deflection of a swept cantilever plate of uniform thickness, using the Rayleigh-Ritz method, by applying the solution to low aspect ratio plates instead of high aspect ratio plates as had been done previously. The Rayleigh-Ritz deflection functions which were used were products of vibration modes of uniform clamped-free and free-free bars.

Deflections were computed, using six terms in the series, for three different loading conditions at sweep angles of 20°, 40°, and 60°. The results, plotted against experimental data in Figures 7 to 24, show that the rate of convergence is satisfactory only for angles of sweep of 20° or less. Since the cases of sweep of 20° or more are of most interest in the application to swept back aircraft wings, it was concluded that the rate of convergence is not satisfactory.

The possibility of improving the rate of convergence of the series solution by solving for the difference between the true deflections and the deflections given by some approximate formula was indicated as the next step in arriving at a satisfactory solution. It was pointed out that the experimental data mentioned above would provide a valuable guide in the formulation of such an approximate formula.

TABLE OF CONTENTS

TABLE OF CONTENTS (Continued)

TABLE OF NOTATIONS

x, y, z Right-handed rectangular coordinate system.

ξ, η Skew coordinate system in the xy-plane.

n, t Local coordinates at the boundary of a plate in the plane of the plate. n is normal to the boundary and t is tangential. The sense of rotation from n to t is the same as from x to y or ξ to η.

q Intensity of distributed lateral load over the surface of a plate, positive in the same direction as positive w.

w Lateral deflection of a plate in the positive z-direction.

P Concentrated lateral load at some point on a plate, positive in the same direction as positive w.

Q_n Lateral shearing force per unit length along the boundary of a plate, positive in the same direction as positive w.

H_{nt} Twisting moment per unit length along the boundary of a plate. The vector of the moment is along the local n-axis, and the direction is taken so that positive $\frac{\partial H_{nt}}{\partial s}$ is in the direction of positive w.

M_n Bending moment per unit length along the boundary of a plate. The vector of the moment is along the local positive t-axis,

TABLE OF NOTATIONS (Continued)

so that positive M puts into tension the side of the plate which faces the direction of positive deflection.

w_o — Approximate deflection function for a plate.

$f_m\left(\frac{\xi}{L}\right)$ — mth mode of vibration of a uniform bar of length L clamped at $\xi = 0$ and free at $\xi = L$.

$g_n(\eta)$ — nth mode of vibration of a uniform bar of length 2 sc. free at both ends.

$h_m\left(\frac{\xi}{L}\right)$ — mth mode of vibration of a uniform bar of length L simply supported at both ends.

a_{mn} — Coefficient of typical term $\frac{1}{\sqrt{L}} f_m\left(\frac{\xi}{L}\right) g_n(\eta)$, or $\frac{1}{\sqrt{L}} h_m\left(\frac{\xi}{L}\right) g_n(\eta)$, in series approximation to plate deflection.

E — Young's modulus.

ν — Poisson's ratio.

t — Plate thickness.

$D = \frac{E t^3}{12(1-\nu)}$ — Plate stiffness factor.

sc. — Semi-chord; half the chord of a wing or the corresponding dimension of a plate of similar planform.

θ — Angle of sweep.

TABLE OF NOTATIONS (Continued)

L	Length along the leading or trailing edge of a wing or the corresponding dimension of a plate of similar planform.
U	Strain energy of bending in a deformed plate.
W	Potential energy lost by the external loads in deforming a plate.
$V=U-W$	Total potential energy of a deformed plate.
G	Modulus of shear.
I	Moment of inertia of the cross-section of a uniform beam, about the neutral axis perpendicular to the plane in which the beam is bent.
J	Polar moment of inertia of the cross-section of a uniform beam about the centroid of the cross-section.

INTRODUCTION

As an approach to the overall problem of stress and deflection distribution in swept aircraft wings of high solidity, the application of the Rayleigh-Ritz method to the deflections of swept cantilever plates of uniform thickness was initiated by Y. C. Fung of the Guggenheim Aeronautical Laboratories, California Institute of Technology, in Air Force Technical Report 5761 - Part I (February 1949). The detailed procedure and the numerical application of the method to the case of large aspect ratio swept plates were presented by the same author in Part II of the same report in June 1949.

The numerical results of Part II showed that the convergence was very poor for large aspect ratios, and it was concluded that the convergence might be improved by applying the method to a plate of small aspect ratio, because the chordwise and spanwise characteristics of the Rayleigh-Ritz deflection functions would then have equal significance in solving for the Rayleigh-Ritz coefficients. Furthermore, the solution for the small aspect ratio plate has the advantage of giving a more exact solution for the critical root section of a large aspect ratio plate when the effects of the outer portions of the latter are replaced by suitable loads at the tip section.

This report extends the work into the case of small aspect ratios. In addition the numerical methods are discussed from a somewhat different approach which to some readers may appear more lucid. The results of the numerical work and an experimental verification are plotted in Figures 7 to 24. A summary of the properties of the deflection functions and many related expressions appears in the appendices.

This method is easily adapted to the problem of the deflection of skew slabs simply supported on two opposite edges and free along the other two edges. This is of interest to Civil Engineers engaged in the design of skew bridges for modern high speed highways. The solution for this problem is given in Part II, but no numerical work has yet been done on it.

PART I

THE RALEIGH-RITZ METHOD

AND ITS

APPLICATION TO CANTILEVER SWEPT PLATES

A. The Rayleigh-Ritz Method

The Rayleigh-Ritz method consists of assuming that some desired deflection pattern can be approximated by a linear combination of deflection functions, each of which satisfies the rigid boundary conditions of the problem, and then finding the coefficients governing this linear combination by minimizing the total potential energy of the deformed body and the external forces. Thus, we may assume that the deflection pattern of a plate whose dimensions, supports, and external loads are specified (e.g. Figure 1) can be approximated by a linear combination of $F_1(x,y), F_2(x,y), F_3(x,y)$, etc. where all the $F_i(x,y)$ satisfy the rigid boundary conditions of the supports. The deflection pattern can immediately be written down in the symbolic form

$$w(x,y) = \sum_i a_i F_i(x,y). \tag{I-1}$$

The problem is now one of finding the most nearly correct values for the a_i's, and the criterion we use is that the total potential energy be minimized.

The total potential energy is the sum of the strain energy of the plate, U, and the potential energy of the external loads, $-W$. It is convenient to choose the zero datum for W to correspond to $U=0$ (unstrained plate). Then W is the sum (or integral) of the products of the external forces and moments by their corresponding deflections

and rotations. We can express the total potential energy as

$$V = U - W. \tag{I-2}$$

Then the value of a_i giving the minimum V is found by equating

$$\frac{\partial V}{\partial a_i} = \frac{\partial (U-W)}{\partial a_i} = 0. \tag{I-3}$$

However, we will find that the expression for U in the case of a plate is such that substitution of equation (I-1) into equation (I-2) will give a quadratic expression in the a_i's. Thus we are faced with the problem of solving a set of linear simultaneous equations in order to find a set of a_i's.

The functions chosen for F_i will usually be an infinite sequence so that if a sufficient number of a_i's are found, the deflection can be found to any desired accuracy. On the other hand, the amount of work involved in solving for the a_i's will go up roughly as the square of the number of a_i's because of the need for solving the simultaneous equations. So a balance between accuracy and facility must be decided upon.

B. Plates Investigated

In the present work, we are concerned with plates which represent idealized aircraft wings (or control surfaces). The planform is in general a parallelogram and the boundary conditions are one edge clamped and the other three edges free. (See Figure 2(a).) In particular we are interested in swept wings of low aspect ratio, so that the parallelogram becomes approximately a rhombus. (See Figure 2(b).) The mathematical treatment of this swept plate is greatly simplified by the use of skew coordinates (ξ, η) shown in Figure 2(b). The basic planform dimensions of the plate are the length of the center-line, L, the semi-

chord, sc., and the angle of sweep, θ . The term "sc." will henceforth be used freely as a unit of length in precisely the same manner as "in." or "ft.", but it should be remembered that, for each plate investigated, one sc. must be evaluated in terms of inches, feet, or some other standard unit of length. By this device, we can take advantage of the numerical brevity of reduction to dimensionless form without losing the physical significance of the expressions encountered.

C. Choice of Deflection Functions

The two ultimate criteria governing the choice of the deflection functions $F_i(\xi,\eta)$ are the ease with which a sufficient number of the constants a_i may be evaluated and the ease with which the deflection at any point on the plate may finally be computed. Both of these considerations call for rapid convergence, but this is a rather intangible property which is a consequence of how closely the assumed functions actually represent the desired deflection pattern.

In some cases, an artificial aid to convergence may be introduced by adding to the solution an additional term, w_o , which is believed to be a fairly close approximation to the answer sought. In this way, the remaining terms, $\sum_i a_i F_i(\xi,\eta)$, are reduced to the role of correction terms and may be expected to be significantly smaller and hence to converge more rapidly. However, the solution in this form, namely

$$w(\xi,\eta) = w_o(\xi,\eta) + \sum_i a_i F_i(\xi,\eta), \qquad \text{(I-4)}$$

will increase the amount of labor involved in evaluating the a_i's. The amount by which this factor offsets the advantage gained by the improved convergence should not be overlooked.

A property which greatly reduces the amount of labor involved

in evaluating the a_i's is orthogonality. This is a general property of vibration modes and hence makes these more desirable than, say, buckling modes. No solution for the modes of vibration of the family of plates covered in this work are known to the writer. Furthermore, it seems reasonable to expect that such a solution, including variation of sweep angle, would be quite complicated. If, however, we take the product of the modes of vibration of two bars whose boundary conditions match those of the plate in the spanwise (ξ) and chordwise (η) directions separately, we will have functions which are reasonably simple and are not affected by variation of the sweep angle, θ . Consequently, we will say

$$a_{mn} F_{mn}(\xi,\eta) = \frac{a_{mn}}{\sqrt{L}} f_m\left(\frac{\xi}{L}\right) g_n(\eta) \qquad \text{(I-5)}$$

where $f_m\left(\frac{\xi}{L}\right)$ is the mth mode of vibration of a bar of length clamped at $\xi = 0$ and free at $\xi = L$, and $g_n(\eta)$ is the nth mode of vibration of a bar of length $2\,sc.$ free at both ends. The factor $\frac{1}{\sqrt{L}}$ is introduced to simplify some of the subsequent expressions. Now we have

$$w(\xi,\eta) = w_0(\xi,\eta) + \frac{1}{\sqrt{L}} \sum_{m,n} a_{mn} f_m\left(\frac{\xi}{L}\right) g_n(\eta). \qquad \text{(I-6)}$$

The value of $w_0(\xi,\eta)$ ought to come from some reasonably similar configuration for which a simple solution is known. For example, for a similar plate of high aspect ratio, the deflection and twist of a simple beam were superimposed (with slight modification to obtain $w = 0$ at $\xi = 0$ for any value of θ) to give w_0 (see Reference 1). However, the usefulness of this approximation was based on the fact that the root and tip triangles (Figure 2(a)), which are

an indication of the variation of the plate from a simple beam, were a small portion of the total area of the plate. In the present case, however, this is not true (Figure 2(b)). Therefore, we will let

$$w_o(\xi, \eta) = 0, \tag{I-7}$$

so that equation (I-6) becomes

$$w(\xi, \eta) = \frac{1}{\sqrt{L}} \sum_{m,n} a_{mn} f_m\left(\frac{\xi}{L}\right) g_n(\eta). \tag{I-6a}$$

We may note at this point that if we take $f_m\left(\frac{\xi}{L}\right)$ and $g_n(\eta)$ as dimensionless quantities, the dimensions of a_{mn} must be $(\text{length})^{3/2}$. Note also that the arguments of f_m and g_n, although not of the same dimensions, are not necessarily inconsistent, since their only function is to indicate position along the length of the bar.

D. Strain Energy

The strain energy of bending for a flat plate, neglecting straining in the plane of the plate, is

$$U = \frac{1}{2} \iint_R D \left\{ \left(\frac{\partial^2 w}{\partial x^2} + \frac{\partial^2 w}{\partial y^2} \right)^2 - 2(1-\nu) \left[\frac{\partial^2 w}{\partial x^2} \frac{\partial^2 w}{\partial y^2} - \left(\frac{\partial^2 w}{\partial x \partial y} \right)^2 \right] \right\} dx\, dy \tag{I-8}$$

for a rectangular coordinate system (Reference 2.) where the double integration is carried out over the entire surface of the plate. The transformation from rectangular coordinates to the skew coordinates of Figure 2(a) is governed by the following equations (see also Figure 3):

$$\left.\begin{aligned} x &= \xi \cos\theta \\ y &= \eta + \xi \sin\theta \end{aligned}\right\} \tag{I-9a}$$

$$\left.\begin{aligned} \xi &= x \sec\theta \\ \eta &= y - x \tan\theta \end{aligned}\right\}. \tag{I-9b}$$

Substituting equation (I-9a) into (I-8), we get

$$U = \frac{1}{2}\int_{-l_{sc.}}^{l_{sc.}}\int_{0}^{L}\frac{D}{\cos^3\theta}\left\{\left(\frac{\partial^2 w}{\partial \xi^2} - 2\sin\theta\,\frac{\partial^2 w}{\partial \xi \partial \eta} + \frac{\partial^2 w}{\partial \eta^2}\right)^2 - 2(1-\nu)\cos^2\theta\left[\frac{\partial^2 w}{\partial \xi^2}\frac{\partial^2 w}{\partial \eta^2} - \left(\frac{\partial^2 w}{\partial \xi \partial \eta}\right)^2\right]\right\} d\xi\, d\eta. \tag{I-10}$$

E. Potential Energy of the External Loads

Using the notation indicated at the beginning of the report, the potential energy lost by the external loads can be written down as

$$W = \int_{-l_{sc.}}^{l_{sc.}}\int_{0}^{L} q(\xi,\eta)\, w(\xi,\eta)\cos\theta\, d\xi\, d\eta - \int M_n(s)\frac{\partial w}{\partial n}(s)\, ds + \int\left(Q_n(s) + \frac{\partial H_{nt}}{\partial s}(s)\right) w(s)\, ds + \sum_i P_i\, w(\xi_i,\eta_i) \tag{I-11}$$

where the line integrals are taken over the free edges of the plate.

F. Derivation of Simultaneous Equations for the a_{mn}'s.

Substitution of equations (I-10), (I-11), (I-6a) and (I-2) into equation (I-3) is a tedious but straightforward procedure which will not be carried out here. In the course of deriving the typical simultaneous equations by this process, substitution of the following properties and defined functions of the vibration modes of the "clamped-free" and "free-free" bars results in enormous simplification of the derivation and all the work which follows.

Orthogonality of vibration modes:

$$\int_0^1 f_m\left(\frac{\xi}{L}\right) f_n\left(\frac{\xi}{L}\right) d\left(\frac{\xi}{L}\right) = \int_{-1}^{1} g_m(\eta)\, g_n(\eta)\, d\eta = \delta_{mn} \tag{I-12}$$

where $\delta_{mn} = 1$ if $m = n$, $\delta_{mn} = 0$ if $m \neq n$. (δ_{mn} is the Kronecker delta.) Note that equation (I-12) also specifies the amplitudes of the vibration modes.

Defined functions of vibration modes:

$$\alpha_{mn}=\int_0^1 f_m''\left(\frac{\xi}{L}\right)f_n''\left(\frac{\xi}{L}\right)d\left(\frac{\xi}{L}\right)=\alpha_{nm} \qquad [1] \qquad \text{(I-13a)}$$

$$\beta_{mn}=\int_0^1 f_m'\left(\frac{\xi}{L}\right)f_n'\left(\frac{\xi}{L}\right)d\left(\frac{\xi}{L}\right)=\beta_{nm} \qquad [1] \qquad \text{(I-13b)}$$

$$\gamma_{mn}=\int_0^1 f_m''\left(\frac{\xi}{L}\right)f_n\left(\frac{\xi}{L}\right)d\left(\frac{\xi}{L}\right) \qquad [1] \qquad \text{(I-13c)}$$

$$\psi_{mn}=\int_0^1 f_m''\left(\frac{\xi}{L}\right)f_n'\left(\frac{\xi}{L}\right)d\left(\frac{\xi}{L}\right) \qquad [1] \qquad \text{(I-13d)}$$

$$\tau_{mn}=\int_0^1 f_m'\left(\frac{\xi}{L}\right)f_n\left(\frac{\xi}{L}\right)d\left(\frac{\xi}{L}\right) \qquad [1] \qquad \text{(I-13e)}$$

$$\varkappa_{mn}=\int_{-lsc.}^{lsc.} g_m''(\eta)\,g_n''(\eta)\,d\eta=\varkappa_{nm} \qquad \left[\frac{1}{L^3}\right] \qquad \text{(I-13f)}$$

$$\lambda_{mn}=\int_{-lsc.}^{lsc.} g_m'(\eta)\,g_n'(\eta)\,d\eta=\lambda_{nm} \qquad \left[\frac{1}{L}\right] \qquad \text{(I-13g)}$$

$$\mu_{mn}=\int_{-lsc.}^{lsc.} g_m''(\eta)\,g_n(\eta)\,d\eta \qquad \left[\frac{1}{L}\right] \qquad \text{(I-13h)}$$

$$\pi_{mn}=\int_{-lsc.}^{lsc.} g_m''(\eta)\,g_n'(\eta)\,d\eta \qquad \left[\frac{1}{L^2}\right] \qquad \text{(I-13i)}$$

$$\zeta_{mn}=\int_{-lsc.}^{lsc.} g_m'(\eta)\,g_n(\eta)\,d\eta \qquad [1] \qquad \text{(I-13j)}$$

where the primes indicate differentiation of $f_m\left(\frac{\xi}{L}\right)$ with respect to $\frac{\xi}{L}$ and of $g_n(\eta)$ with respect to η, and the expressions in brackets $[\ ]$ give the dimensions of the functions.

$$\alpha_{mn}=\varkappa_{mn}=0 \quad \text{if } m\neq n. \qquad \text{(I-14)}$$

Proof of equations (I-14) and further evaluation of equations (I-13) will be discussed in Appendix I.

$$\sqrt{L}\frac{\partial V_o}{\partial a_{mn}} = \sqrt{L}\frac{\partial W}{\partial a_{mn}} = -\cos\theta\int_{-l_{sc.}}^{l_{sc.}}\int_0^L q(\xi,\eta) f_m\left(\frac{\xi}{L}\right) g_n(\eta)\, d\xi\, d\eta$$
$$+\int M_n \frac{\partial(f_m g_n)}{\partial n}\, ds - \int\left(Q_n + \frac{\partial H_{nt}}{\partial s}\right) f_m g_n\, ds \qquad \text{(I-15)}$$
$$-\sum_i P_i f_m\left(\frac{\xi_i}{L}\right) g_n(\eta_i).$$

This expression includes all the terms in equation (I-3) that do not contain a factor of one of the a_{mn}'s. Hence, it is (except for a constant factor) the constant term for the typical simultaneous equation. (If an approximate deflection, w_o, is used, $\sqrt{L}\frac{\partial V_o}{\partial a_{mn}}$ contains an additional series of terms which contain w_o. For this complete form of $\sqrt{L}\frac{\partial V_o}{\partial a_{mn}}$, see Eq. 4.2:21, Reference 1.)

The typical simultaneous equation, derived through the procedure outlined above is

$$\frac{L^2\cos^3\theta}{D}\frac{\partial U}{\partial a_{mn}} = \sum_{i,j} a_{ij}\Big[2\left(1+\sin^2\theta-\nu\cos^2\theta\right)\beta_{im}\lambda_{nj}$$
$$+\left(\sin^2\theta+\nu\cos^2\theta\right)\left(\gamma_{im}\mu_{nj}+\gamma_{mi}\mu_{jn}\right) \qquad \text{(I-16)}$$
$$-2\sin\theta\left\{\frac{1}{L}\left(\psi_{im}\zeta_{nj}+\psi_{mi}\zeta_{jn}\right)+L\left(\tau_{im}\pi_{nj}+\tau_{mi}\pi_{jn}\right)\right.$$
$$\left.+a_{mn}\left[\frac{s_{c.}\alpha_{mm}}{L^2}+L^2\alpha_{nn}\right]\right] = -\frac{L^2\cos^3\theta}{D}\frac{\partial V_o}{\partial a_{mn}}.$$

PART II

APPLICATION TO THE PROBLEM OF A SKEW HIGHWAY BRIDGE

A. The Skew Highway Bridge

A problem of increasing interest to Civil Engineers, in the design of modern high speed highways, is that of the deflections (and stresses) of skew highway bridges. These structures may be idealized into skew slabs simply supported along two edges and free along the other two edges. Thus we have essentially the same problem as the built-in flat plate discussed above with two of the boundary conditions changed. It will be convenient to translate the origin of the skew coordinates to the center of the plate. (See Figure 4.) In addition it is not uncommon to have curbing parallel to the free edges of the span, and we will add a term to the energy expression to account for this.

B. Deflection Functions

In this case, we replace the modes of vibration of a clamped-free bar by those of a bar which is simply supported at both ends. Actually these modes are pure sinusoidal in form, but we will call them $h_m\left(\frac{\xi}{L}\right)$ for the purpose of symbolic notation. With $w_0(\xi,\eta)=0$, we have

$$w(\xi,\eta) = \frac{1}{\sqrt{L}} \sum_{m,n} a_{mn}\, h_m\left(\frac{\xi}{L}\right) g_n(\eta). \qquad \text{(II-1)}$$

C. Strain Energy and Potential Energy

We will say

$$U = U_1 + U_2 \qquad \text{(II-2)}$$

where U_1 is the strain energy of the plate, and U_2 is the strain energy of the curbing. In this case,

$$U_1 = \frac{1}{2}\int_{-lsc.}^{lsc.}\int_{-\frac{L}{2}}^{\frac{L}{2}} \frac{D}{\cos^3\theta}\left\{\left(\frac{\partial^2 w}{\partial \xi^2} - 2\sin\theta\frac{\partial^2 w}{\partial \xi \partial \eta} + \frac{\partial^2 w}{\partial \eta^2}\right)^2 - 2(1-\nu)\cos^2\theta\left[\frac{\partial^2 w}{\partial \xi^2}\frac{\partial^2 w}{\partial \eta^2} - \left(\frac{\partial^2 w}{\partial \xi \partial \eta}\right)^2\right]\right\} d\xi\, d\eta \qquad \text{(II-3)}$$

which, except for the limits of integration, is identical to U for the cantilever plate (equation (I-10)). Treating the curbing by the classical beam theory, we have

$$U_2 = \frac{1}{2}\int_S M(\xi)\, d\left(\frac{dw}{d\xi}\right) + \frac{1}{2}\int_S T(\xi)\, d\left(\frac{dw}{d(\eta\cos\theta)}\right) \qquad \text{(II-4)}$$

where the line integral is taken along whatever curbing exists, and $M(\xi)$ and $T(\xi)$ are the bending moment and twisting moment, respectively, experienced by the curbing. Substituting

$$M(\xi) = E\,I(\xi)\,\frac{d^2 w}{d\xi^2} \qquad \text{(II-5a)}$$

and

$$T(\xi) = G\,J(\xi)\,\frac{d}{d\xi}\left(\frac{dw}{d(\eta\cos\theta)}\right), \qquad \text{(II-5b)}$$

we obtain

$$U_2 = \frac{1}{2}\int_S \left\{EI(\xi)\left(\frac{d^2 w}{d\xi^2}\right)^2 + \frac{GJ(\xi)}{\cos^2\theta}\left(\frac{d^2 w}{d\xi\, d\eta}\right)^2\right\} d\xi\,. \qquad \text{(II-6)}$$

The potential energy of the external loads is the same as before, except for the change in the limits of the surface integral as typified in Equation (II-3). With this change, equation (I-II) may be used here.

D. Derivation of Simultaneous Equations for the a_{mn}'s.

The process of obtaining the typical simultaneous equation -- by substituting equations (II-2), (II-3), (II-6), (I-11), and (I-2) into (I-3) -- can again be simplified by the use of the properties and

Defined functions of the vibration modes. We introduce the following new properties and expressions:

Orthogonality:

$$\int_{-\frac{1}{2}}^{\frac{1}{2}} h_m\left(\frac{\xi}{L}\right) h_n\left(\frac{\xi}{L}\right) d\left(\frac{\xi}{L}\right) = \delta_{mn} \qquad \text{(II-7)}$$

where $\delta_{mn} = 1$ if $m = n$, $\delta_{mn} = 0$ if $m \neq n$.

Defined functions:

$$\Delta_{mn} = \int_{-\frac{1}{2}}^{\frac{1}{2}} h_m''\left(\frac{\xi}{L}\right) h_n''\left(\frac{\xi}{L}\right) d\left(\frac{\xi}{L}\right) = \Delta_{nm} \qquad [1] \qquad \text{(II-8a)}$$

$$\varepsilon_{mn} = \int_{-\frac{1}{2}}^{\frac{1}{2}} h_m'\left(\frac{\xi}{L}\right) h_n'\left(\frac{\xi}{L}\right) d\left(\frac{\xi}{L}\right) = \varepsilon_{nm} \qquad [1] \qquad \text{(II-8b)}$$

$$\sigma_{mn} = \int_{-\frac{1}{2}}^{\frac{1}{2}} h_m''\left(\frac{\xi}{L}\right) h_n\left(\frac{\xi}{L}\right) d\left(\frac{\xi}{L}\right) \qquad [1] \qquad \text{(II-8c)}$$

$$\varphi_{mn} = \int_{-\frac{1}{2}}^{\frac{1}{2}} h_m''\left(\frac{\xi}{L}\right) h_n'\left(\frac{\xi}{L}\right) d\left(\frac{\xi}{L}\right) \qquad [1] \qquad \text{(II-8d)}$$

$$\omega_{mn} = \int_{-\frac{1}{2}}^{\frac{1}{2}} h_m'\left(\frac{\xi}{L}\right) h_n\left(\frac{\xi}{L}\right) d\left(\frac{\xi}{L}\right) \qquad [1] \qquad \text{(II-8e)}$$

where the primes indicate differentiation with respect to $\frac{\xi}{L}$, and the expressions in brackets [ ] indicate the dimensions of the expression.

$$\Delta_{mn} = \varepsilon_{mn} = \sigma_{mn} = 0 \quad \text{if } m \neq n$$
$$\varphi_{mn} = \omega_{mn} = 0, \quad \text{any } m, n. \qquad \text{(II-9)}$$

Proof of equations (II-9) and further evaluation of equations (II-8) will be discussed in Appendix I.

$$\sqrt{L}\,\frac{\partial V_0}{\partial a_{mn}} = -\sqrt{L}\,\frac{\partial W}{\partial a_{mn}} = \text{same as equation (I-15) with limits of integration changed. [F]} \qquad \text{(II-10)}$$

This is true for $w_0 = 0$ only.

The term corresponding to U_1 in the typical equation is similar to the term given for U in equation (I-16). Retracing the derivation of equation (I-16), it is seen that the functions given in equations (I-13 a,b,c,d,e) are replaced by the corresponding ones in equations (II-8a,b,c,d,e) resulting in

$$\frac{L^2\cos^3\theta}{D}\frac{\partial U_1}{\partial a_{mn}} = a_{mn}\left[\frac{\text{sc.}\,\Delta_{mm}}{L^2} + L^2\varkappa_{nn}\right]$$

$$+\sum_{m,j} a_{mj}\left[2\left(1+\sin^2\theta-\nu\cos^2\theta\right)\varepsilon_{mnn}\lambda_{nj}+\left(\sin^2\theta+\nu\cos^2\theta\right)\left(\tau_{mnn}\mu_{nj}+\tau_{mnn}\mu_{jn}\right)\right]. \qquad \text{(II-11)}$$

The brief form of this expression is due to the vanishing of several functions as indicated in equation (II-9).

The term corresponding to U_2 will be derived here since this has not been done previously and because the derivation will be illustrative of the way in which equations (I-16) and (II-11) were obtained.

From equations (II-6) and (II-1),

$$U_2 = \frac{1}{2}\int_S EI(\xi)\left(\frac{1}{\sqrt{L}}\sum_{i,j} a_{ij}\frac{\partial^2 h_i\left(\frac{\xi}{L}\right)}{\partial\xi^2} g_j(\eta)\right)^2 d\xi$$

$$+\frac{1}{2}\int_S \frac{GJ(\xi)}{\cos^2\theta}\left(\frac{1}{\sqrt{L}}\sum_{i,j} a_{ij}\frac{\partial h_i\left(\frac{\xi}{L}\right)}{\partial\xi}\frac{\partial g_j(\eta)}{\partial\eta}\right)^2 d\xi$$

$$\frac{\partial U_2}{\partial a_{mn}} = \int_S EI(\xi)\frac{1}{L}\frac{\partial^2 h_m\left(\frac{\xi}{L}\right)}{L^2\partial\left(\frac{\xi}{L}\right)^2} g_n(\eta)\sum_{i,j} a_{ij}\frac{\partial^2 h_i\left(\frac{\xi}{L}\right)}{L^2\partial\left(\frac{\xi}{L}\right)^2} g_j(\eta)\,d\xi$$

$$+\int_S \frac{GJ\left(\frac{\xi}{L}\right)}{\cos^2\theta}\frac{1}{L}\frac{\partial h_m\left(\frac{\xi}{L}\right)}{L\partial\left(\frac{\xi}{L}\right)}\frac{\partial g_n(\eta)}{\partial\eta}\sum_{i,j} a_{ij}\frac{\partial h_i\left(\frac{\xi}{L}\right)}{L\partial\left(\frac{\xi}{L}\right)}\frac{\partial g_j(\eta)}{\partial\eta}\,d\xi.$$

If the curbing is taken in the form of any number of uniform beams, parallel to the free edges (i.e., parallel to the η-axis, we may say

$$EI(\xi) = \text{const.} \quad \text{for } \eta = \eta_k$$
$$GJ(\xi) = \text{const.} \quad \text{for } \eta = \eta_k$$

where η_k is the value of η locating the k^{th} curb. (For the special case of curbing along both free edges only, $\eta_1 = -1.0$ sc., $\eta_2 = 1.0$ sc., and $k = 1,2$ only.)

Then

$$\frac{\partial U_2}{\partial a_{mn}} = \sum_k \frac{EI(\eta_k)}{L^4} g_n(\eta_k) \sum_{i,j} a_{ij}\, g_j(\eta_k) \underbrace{\int_{-\frac{1}{2}}^{\frac{1}{2}} h_m''\left(\frac{\xi}{L}\right) h_i''\left(\frac{\xi}{L}\right) d\left(\frac{\xi}{L}\right)}_{\Delta_{mi}}$$
$$+ \sum_k \frac{GJ(\eta_k)}{L^2 \cos^2\theta} g_n'(\eta_k) \sum_{i,j} a_{ij}\, g_j'(\eta_k) \underbrace{\int_{-\frac{1}{2}}^{\frac{1}{2}} h_m'\left(\frac{\xi}{L}\right) h_i'\left(\frac{\xi}{L}\right) d\left(\frac{\xi}{L}\right)}_{\varepsilon_{mi}}.$$

Recalling that $\Delta_{mn} = \varepsilon_{mn} = 0$ if $m \neq n$, this reduces to

$$\frac{\partial U_2}{\partial a_{mn}} = \frac{\Delta_{mm}}{L^4} \sum_k EI(\eta_k) g_n(\eta_k) \sum_{m,j} a_{mj}\, g_j(\eta_k)$$
$$+ \frac{\varepsilon_{mm}}{L^2 \cos^2\theta} \sum_k GJ(\eta_k) g_n'(\eta_k) \sum_{m,j} a_{mj}\, g_j'(\eta_k).$$

Finally, $\frac{L^2 \cos^3\theta}{D} \frac{\partial U_2}{\partial a_{mn}} = \frac{\Delta_{mm} \cos^3\theta}{L^2 D} \sum_k EI(\eta_k) g_n(\eta_k) \sum_{m,j} a_{mj}\, g_j(\eta_k)$

$$+ \frac{\varepsilon_{mm} \cos\theta}{D} \sum_k GJ(\eta_k) g_n'(\eta_k) \sum_{m,j} a_{mj}\, g_j'(\eta_k). \qquad \text{(II-12)}$$

The symbol $\sum_{m,j}$ means that only those members of the set of ij's for which i = m are included. From equations (II-11) and (II-12) it may be noted that in the typical equation for the a_{ij}'s corresponding to $\frac{\partial U}{\partial a_{mn}}$, only those a_{ij}'s for which i = m will have coefficients which are $\neq 0$. This will give, for example, four sets of four simultaneous equations each in place of one set of sixteen simultaneous equations, which reduces the computational labor considerably.

Finally, we have for the typical equation

$$\frac{L^2\cos^3\theta}{D}\frac{\partial U_1}{\partial a_{mn}} + \frac{L^2\cos^3\theta}{D}\frac{\partial U_2}{\partial a_{mn}} = \frac{L^2\cos^3\theta}{D}\frac{\partial W}{\partial a_{mn}} \; ; \left[L^{\frac{1}{2}}\right] \qquad \text{(II-13)}$$

where the partial derivatives are evaluated by means of equations (II-11), (II-12), and (II-10) respectively.

PART III

COMPUTATIONAL PROCEDURES AND RESULTS

A. Simplification of the Computations

The numerical application of this method involves a rather extensive program of computing. However, the writer has found it possible to arrange and subdivide the operations in such a way that the amount of labor involved is materially reduced and so that the reasoning required during most of the operations is at a minimum. This latter circumstance makes it possible to have the work done, for the most part, by computers who are entirely unfamiliar either with the problem itself or with the methods of matrix algebra (which are used to advantage in this process). The techniques arrived at will be described here for the purpose of facilitating similar work.

B. Linear Combinations of Matrices

Twice in the application of this method it is necessary to obtain linear combinations of matrices. Therefore, a process by which this can easily be done will be described in general terms.

If $[A], [B], \cdots$ represent a sequence of matrices, the sum may be written symbolically as

$$[S] = [A] + [B] + \cdots . \qquad \text{(III-1)}$$

A linear combination of the same matrices is a generalization of addition, namely

$$[N] = a[A] + b[B] + \cdots \qquad \text{(III-2)}$$

where a, b, $\cdots$ are constants.

In either of these operations, it is necessary that the positions of the terms in the different matrices be described by the same coordinate system. For addition, all the terms (one for each matrix) whose positions are described by some two coordinates may be added and the sum taken as the term corresponding to the same two coordinates in the sum matrix $[S]$. The linear combination may be found by multiplying <u>each</u> term of each matrix by the corresponding constant and adding the resulting matrices by the procedure indicated above. A slightly different way of viewing this process is simply to sum the matrices, multiplying each term by its corresponding constant before adding it in.

If, for example, any term of the matrix $[A]$ is represented symbolically by A_{pq} where p and q are the two coordinates of the position associated with this term, the term of the sum matrix associated with the coordinates p and q is

$$S_{pq} = A_{pq} + B_{pq} + \cdots \tag{III-3}$$

and the term of the linear combination of the matrices associated with p and q is

$$N_{pq} = a A_{pq} + b B_{pq} + \cdots \tag{III-4}$$

It is customary for the first subscript, p , to indicate the row and for the second subscript, q , to indicate the column.

In the numerical calculation of a linear combination of matrices, the following steps should be carried out:

1. Write each matrix on a separate sheet of some standard tabulating form (uniform columns and uniform rows). Leave a

blank line between rows and a blank column between columns. Every term (one for each matrix, and some terms may be zero!) corresponding to some particular pair of coordinates should be entered in exactly the same space in its own matrix sheet, so that when the sheets are stacked neatly these terms will be directly above and below one another.

2. Prepare a blank matrix sheet (columns and rows labeled) according to the same scheme.

3. On another sheet of the same type, write the factors of the various matrices (a, b, ...) in order in a single horizontal row with a blank column between adjoining factors. Make a horizontal fold in this sheet in the middle of the blank line above the row of factors, folding the upper portion under.

4. To find, for example, the value of N_{1j} (where p = 1 indicates the 1st row and q = j indicates the jth column)

(a) Fold each matrix sheet vertically in the middle of the blank column between the (j-1)th and jth columns, folding the left portions under.

(b) Stack them vertically with the $[A]$ sheet at the bottom, the $[B]$ above it, and so on.

(c) Starting with all the folded edges together, move each sheet two columns to the right with respect to the one immediately below it, thereby exposing the jth column of each matrix, arranged in order with A_{pj} at the left, B_{pj} next to it, and so on.

(d) Place the sheet containing the factors below the first row of the arrangement in (c) so that a is below A_{1j}, b

is below B_{1j} , etc.

(e) N_{1j} may now be computed according to equation (III-4) in a single operation with a Friden (or similar type) desk calculator and the result entered in the corresponding space on the blank matrix sheet.

5. Move the sheet containing the factors down two lines so that a is below A_{2j} , etc., and repeat step 4(e) above for N_{2j} . The column may be completed in this way. Figure 5 shows the arrangement of these sheets for the computation of N_{21} when four square matrices of nine terms each are being combined.

6. Repeat steps 4 and 5 above for each other column in turn, completing the linear combination of the matrices.

7. If more than one linear combination is to be made, the factors corresponding to the other combinations may be entered below a, b, ... on the sheet mentioned in step 3 above, with a blank line between sets of factors, and the sheet folded in the middle of the blank line above the row of factors being used.

C. Setting Up the Coefficient Matrices

Looking at equations (I-16) and II-13), in which all the terms on the left contain one of the a_{mn}'s and all the terms on the right are constants, one can see that the complete coefficient matrices for these sets of simultaneous equations can be obtained by linear combinations of matrices whose typical terms are $(\beta_{im}\lambda_{nj})$, $(\gamma_{im}\mu_{nj}+\gamma_{ni}\mu_{jn})$, etc. where the pair of subscripts m and n identify the row and the pair i and j identify the column with which any term is associated. The factors of these

matrices are $2(1+\sin^2\theta-\nu\cos^2\theta)$, $(\sin^2\theta+\nu\cos^2\theta)$, etc. respectively. Matrices whose terms are of the type $(\gamma_{im}\mu_{nj}+\gamma_{mi}\mu_{jn})$ can first be formed by adding two matrices whose typical terms are $(\gamma_{im}\mu_{nj})$ and $(\gamma_{mi}\mu_{jn})$ respectively.

The constant terms on the right side do not involve matrix methods, and are evaluated merely by performing the indicated operations. Formulas for some functions which may be needed in the foregoing process are given in Appendices II and III.

D. Solution of the Equations

Since the coefficient matrices are functions of the plate and not of the external loads on the plate, it is desirable to solve the equations by the matrix inversion method. Once the matrix is inverted the solution for any loading condition may be obtained by evaluating the constant terms for that loading and postmultiplying the inverse matrix by the column matrix of the constant terms.

In standard matrix algebra notation, this process is described symbolically as follows:

The entire set of simultaneous equations is written

$$\left[N_{(mn)(ij)}\right]\left\{a_{(ij)}\right\}=\left\{m_{(mn)}\right\}. \qquad \text{(III-5)}$$

By definition, the inverse matrix $\left[N_{(mn)(ij)}\right]^{-1}$ has the property

$$\left[N_{(mn)(ij)}\right]^{-1}\left[N_{(mn)(ij)}\right]=\left[1\right] \qquad \text{(III-6)}$$

where $\left[1\right]$ is a unit matrix.

hence,

$$\left\{ a_{(ij)} \right\} = \left[N_{(mn)(ij)} \right]^{-1} \left\{ m_{(mn)} \right\} \qquad \text{(III-7)}$$

The matrix inversion may be accomplished by the most convenient means available. (The straightforward check afforded by equation (III-6) emphasizes this fact.) In addition to the standard method (Reference 3), analogue and digital computing methods are available in many industrial and research centers. For this report, the inversion was done by a modified Crout method (Reference 4) contained in a private communication from the Consolidated Engineering Corporation, Pasadena, California.

E. Final Solution

After finding the a_{mn}'s, the deflections are found from equation (I-6a) or (II-1), in matrix form, by a linear combination of matrices whose typical terms are $f_m\left(\frac{\xi_p}{L}\right) g_n(\eta_q)$ and whose corresponding factors are $\frac{a_{mn}}{\sqrt{L}}$. p and q are the coordinates of the matrices and ξ_p and η_q are the corresponding values of the coordinates of the plate. The method of linear combinations of matrices has been described below.

F. Particular Cases Computed

Only the case of the small aspect ratio cantilever plate was solved numerically. At sweep angles of 20 degrees, 40 degrees, and 60 degrees, three types of loading were used. They were (1) uniform surface loading, (2) uniform shear along the tip section $\xi = L$, and (3) torsion at the tip section. (See Figure 6.) This choice was based on the belief that most loads experienced by the root section of a swept wing (or a

swept control surface) could be approximated by some combination of these three types. Sets of six coefficients (a_{mn}'s) were found in each case.

G. Experimental Program

The numerical values used in the calculations were those applicable to a set of plates which were tested under the writer's supervision by the GALCIT 57 Experimental Section at the California Institute of Technology. The dimensions of these plates were $L = 18$ in., sc. = 9 in., t = 1/4 in., and of course $\theta = 20^\circ$, 40°, and 60° respectively. The material was Alcoa Spec.-24ST-4, AN-A-12 whose elastic properties are $E = 10.2 \times 10^6$ psi. and $\nu = .32$. The experimental results are accurate to within 0.003 inches. Figures 7 to 24 inclusive give cross-plots of both the experimental and calculated results. Agreement between the two sets of data was good for $\theta = 20^\circ$ but dropped off alarmingly as θ increased. Further discussion of these results and their implications appears later.

H. Method of Approximating Continuous Shear Loadings

Figures 25, 26, and 27 are photographs of typical test set-ups for each type of loading. These pictures show the way in which the shear loadings along the tip were approximated with modified whiffletrees.

The tip section was divided into ten equal segments and a load was applied at the center of each segment equal to the total load which that segment would sustain under the continuous loading conditions being approximated. The geometry of the whiffletrees was worked out to give the desired distribution of the total deadweight loading. The calculations were then made to agree with this condition by using only the last term in equation (I-11) with one value of the index "i" corresponding

to each concentrated load.

The values of $f_m\left(\frac{\xi_i}{L}\right)$ used in substituting equation (I-6a) into equation (I-11) were also modified to account for the distance (along a line of η = const.) from the application of the load to the tip section itself. The perpendicular distance from the center of the holes to the tip of the plate was in all cases 0.06 inches. Therefore $\Delta\xi$ = -(0.06 in.) sec θ or $\Delta\left(\frac{\xi}{L}\right)$ = -0.00333 sec θ . Using the values of the first derivatives of $f_m\left(\frac{\xi}{L}\right)$ for $\frac{\xi}{L}$ = 1.0,

$$f_m\left(\frac{\xi_i}{L}\right) = f_m(1) + f_m'(1)\cdot\Delta\left(\frac{\xi}{L}\right).$$

Numerical tables of all the major steps in the computing are contained in Reference 5.

In Figure 6b, F_Q and F_K are concentrated loads with the dimensions $[F]$. They are related to the continuous loadings of Figure 6a by the following equations.

$$Q\cdot(2sc.) = 10\,F_Q$$

$$\therefore F_Q = \tfrac{1}{5}\,Q\,sc. \qquad \text{(III-8)}$$

$$K = \frac{Q}{\eta} = \frac{F_K/0.2sc.}{0.1\,sc.} = \frac{3F_K/0.2sc.}{0.3\,sc.} = \cdots = \frac{9F_K/0.2sc.}{0.9sc.}$$

$$\therefore F_K = \frac{1}{50}\,k\,sc.^2 . \qquad \text{(III-9)}$$

It is worth noting that the total shear at the tip section equals $10\,F_Q$ and the total torque equals $2[(F_k)(.1sc.) + (3F_k)(.3sc.) + (5F_k)(.5sc.) + (7F_k)(.7sc.) + (9F_k)(.9sc.)] = 33\,F_k\,sc.$

PART IV

DISCUSSION AND CONCLUSIONS

This investigation was an attempt to predict by a general theoretical method the deflections under load of the root section of a swept-back wing idealized into a flat plate of uniform thickness. The choice of a plate of small aspect ratio was made in order to concentrate the spanwise characteristics of the Rayleigh-Ritz deflection functions into the region of the root, in the hope of improving the convergence of the solution, replacing the outer portion of the wing by suitable loads at the tip section of the small aspect ratio plate.

The type of deflection functions chosen, having suitable properties of orthogonality, could surely be depended upon to converge directly to any known deflection pattern satisfying the same rigid boundary conditions and to give results to any desired accuracy if sufficient terms were taken. The a_{mn}'s found in this way would merely be the Fourier coefficients of the expansion of $w(\xi, \eta)$ in a series of terms of the type $\frac{1}{\sqrt{L}} f_m\left(\frac{\xi}{L}\right) g_n(\eta)$. However, when the deflection pattern itself is the unknown and the coefficients of the various terms are evaluated by some additional criterion (the minimization of the total potential energy) we have no assurance that the series of terms in the answer will converge where we want it to, namely, at the true deflection pattern. Comparison of the calculated and experimental results in Figures 7 to 24 indicates that the process converges to satisfactory values at 20° sweep (and probably less sweep) but that there is an alarming drift from the true deflection values as the sweep increases. Since the structural considerations of aircraft wings are affected most significantly by sweep

if the angle of sweep is greater than 20°, it must be concluded that the convergence is unsatisfactory.

In the presence of this situation, it becomes apparent that an approximate deflection function, w_o , which was discarded earlier, has an indispensible role in a satisfactory solution. An empirical function, which is nowhere more than say 5% or 10% in error at any point on the plate for any angle of sweep would reduce the remaining terms $(\frac{1}{\sqrt{L}} \sum a_{mn} f_m g_n)$ to correction terms which would then converge much more quickly to the actual deflection pattern. Using the results of the experimental program conducted for this series of plates, the possibility of formulating a satisfactory empirical function is greatly increased. While the time limitations under which this report was prepared did not permit of pursuing this possibility, this next step toward a satisfactory solution of the problem is clearly indicated.

It is to be noted that the addition of w_o does not alter the coefficient matrices or their inversions. Reference 1 gives a group of functions of w_o to be <u>added</u> to the constant terms m_{mn} already found. When the a_{mn}'s are found from these new constant terms, the deflections themselves are found from equation (I-6) rather than (I-6a).

REFERENCES

1. Fung, Y. C.: Theoretical and Experimental Effect of Sweep upon the Stress and Deflection Distribution in Aircraft Wings of High Solidity. Part II - Stress and Deflection Analysis of Swept Plates. AFTR 5761 - II. June 1949.

2. Timoshenko, S.: Theory of Plates and Shells. McGraw-Hill Book Company, (1940).

3. Frazer, R. A.; Duncan, W. J.; and Collar, A. R. : Elementary Matrices. The MacMillan Company, (1946)

4. Crout, P. D.: A Short Method of Evaluating Determinants and Solving Systems of Linear Equations. Transactions of the AIEE, (1941), Vol. 60, p. 1235.

5. Wechsler, J. W. : Theoretical and Experimental Effect of Sweep upon the Stress and Deflection Distribution in Aircraft Wings of High Solidity. Part V - An Investigation of the Application of the Rayleigh-Ritz Method to the Deflections of a Small Aspect Ratio Swept Plate of Uniform Thickness. AFTR 5167 - V. June 1950.

6. Lord Rayleigh (J. W. Strutt): The Theory of Sound. Dover Publications, (1945), Vol. I, Chapter 6.

APPENDICES

APPENDIX I - PROPERTIES OF VIBRATION MODES OF UNIFORM BARS

A. General Forms of Solution

The classical treatise on the lateral vibration of bars is to be found in Reference 6. In the present work, we will present some of the basic equations and the special form in which they were utilized both for numerical computation and for evaluating the defined functions of the modes.

Neglecting the contribution to the kinetic energy of a vibrating bar due to the rotational motion of the sections of the bar, assuming a harmonic dependence of the deflections upon time, and separating the variable of time from that of position along the bar, the fundamental differential equation for the vibration modes of a uniform bar is

$$\frac{d^4u}{dx^4} = \frac{m^4}{l^4} u \qquad \text{(AI-1)}$$

where u is the value of the mode at coordinate x along the bar, m is an abstract number, and l is the length of the bar.

The general solution to this equation is of the form

$$u = A \cos m\frac{x}{l} + B \sin m\frac{x}{l} + C \cosh m\frac{x}{l} + D \sinh m\frac{x}{l} . \qquad \text{(AI-2)}$$

The four arbitrary constants may be solved for by substituting two boundary conditions for each end of the bar in question into equation (AI-2). However, since the boundary conditions are homogeneous (of the type $\frac{d^n u}{dx^n} = 0$), the equations for A, B, C, and D will be homogeneous linear simultaneous equations (no constant terms). In this case, we equate the determinant of the coefficients to zero and solve the resulting equation for m . This equation is called the characteristic equation and the set of discrete values of m satisfying

it are the characteristic values or eigenvalues. Substituting any of the characteristic values of m into the simultaneous equations, we can obtain only the ratios between A, B, C, and D, indicating that the amplitudes of the modes are arbitrary.

B. Particular Cases Used in the Present Work

1. Clamped-Free Bar of Length L :

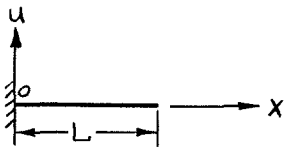

The boundary conditions are

$$u(\text{deflection}) = \frac{du}{dx}(\text{slope}) = 0 \quad \text{at} \quad x = 0$$
$$\frac{d^2u}{dx^2}(\text{moment}) = \frac{d^3u}{dx^3}(\text{shear}) = 0 \quad \text{at} \quad x = L \qquad \text{(AI-3)}$$

giving the characteristic equation

$$\cos p_m \cosh p_m + 1 = 0 \qquad \text{(AI-4)}$$

where p is the notation we will assign to the mth characteristic value corresponding to a clamped-free bar. If equation (AI-4) is written in the form

$$\cosh p_m = -\sec p_m \qquad \text{(AI-4a)}$$

and plotted graphically, it can be seen that p_m may be written in the form

$$p_m = (2m-1)\frac{\pi}{2} + (-1)^{m+1}\alpha_m \qquad \text{(AI-5)}$$

where α_m is a small positive number. In reference 6, the p_m 's are evaluated via this approach. A useful relationship derived in the process is presented here:

$$\cot \frac{\alpha_m}{2} = e^{p_m}. \qquad \text{(AI-6)}$$

The solution is

$$f_m\left(\frac{x}{L}\right) = -\cos\frac{p_m x}{L} + \cosh\frac{p_m x}{L} + \sigma_m\left(\sin\frac{p_m x}{L} - \sinh\frac{p_m x}{L}\right) \qquad \text{(AI-7a)}$$

or

$$f_m\left(\frac{x}{L}\right) = \frac{1}{\gamma_m}\left\{-\sqrt{2}\cos\left[\frac{p_m x}{L} + \frac{\pi}{4} + (-1)^m\frac{\alpha_m}{2}\right] + \left[(-1)^{m+1}e^{-p_m\left(1-\frac{x}{L}\right)} + e^{-p_m\frac{x}{L}}\right]\cos\frac{\alpha_m}{2}\right\} \qquad \text{(AI-7b)}$$

where

$$\sigma_m = \frac{\cos p_m + \cosh p_m}{\sin p_m + \sinh p_m} \qquad \text{(AI-8a)}$$

and

$$\gamma_m = \cos\frac{\alpha_m}{2} + (-1)^{m+1}\sin\frac{\alpha_m}{2}. \qquad \text{(AI-8b)}$$

The replacement of u by f_m indicates that the function has been normalized according to equation (I-12) and the additional criterion

$$f_m(1) = (-1)^{m+1}\left|f_m(1)\right|. \qquad \text{(AI-9)}$$

Equation (AI-7a) is convenient for evaluating functions such as those in equation (I-13), while equation (AI-7b) is useful for numerical computation of the modes themselves.

2. Free-Free Bar of Length 2 sc.:

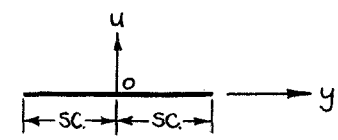

The boundary conditions are

$$\frac{d^2u}{dy^2} = \frac{d^3u}{dy^3} = 0 \quad \text{at} \quad y = \pm 1\,\text{sc.} \qquad \text{(AI-10)}$$

giving the characteristic equation

$$\cos 2q_n \cosh 2q_n = 1 \qquad \text{(AI-11a)}$$

which is identically equal to

$$(\tanh q_n - \tan q_n)(\tanh q_n + \tan q_n) = 0 \qquad \text{(AI-11b)}$$

where $2q_n$ replaces m in the notation for the nth characteristic value for a free-free bar. In this case,

$$q_n = (2n-1)\frac{\pi}{4} + (-1)^n \beta_n \qquad \text{(AI-12)}$$

where β_n is a small positive number. Similar to equation (AI-6), there exists a relationship

$$\cot \beta_n = e^{2q_n}. \qquad \text{(AI-13)}$$

(It should be noted that the $2q_n$ and $2\beta_n$ used here correspond to m and β in Reference 6 if the index is reduced one interger, e.g. $2q_n = m_{n-1}$.) Disregarding for the time being the cases $n = 0, 1$, when n is even, the second factor in equation (AI-11b) equals zero, i.e.

$$\tanh q_n + \tan q_n = 0 \qquad \text{(AI-11c)}$$

giving the normalized solutions

$$g_n(y) = (-1)^{\frac{n}{2}} \frac{\cos q_n \cosh q_n \frac{y}{sc.} + \cosh q_n \cos q_n \frac{y}{sc.}}{\sqrt{2}\cos q_n \cosh q_n} \qquad \text{(AI-14a)}$$

$$= \frac{\cos q_n \cosh q_n \frac{y}{sc.} + \cosh q_n \cos q_n \frac{y}{sc.}}{\sqrt{\cosh^2 q_n + \cos^2 q_n}} \qquad \text{(AI-14b)}$$

$$= \frac{1}{\sqrt{1+\sin 2\beta_n}} \left[\cos q_n \frac{y}{sc.} + (-1)^{\frac{n}{2}} \frac{\cos \beta_n}{\sqrt{2}} \left(e^{-q_n\left(1-\frac{y}{sc.}\right)} + e^{-q_n\left(1+\frac{y}{sc.}\right)}\right)\right] \qquad \text{(AI-14c)}$$

$(n>0, \text{even})$

When n is odd,

$$\tanh q_n - \tan q_n = 0 \qquad \text{(AI-11d)}$$

giving

$$g_n(y) = (-1)^{\frac{n-1}{2}} \frac{\sin q_n \sinh q_n \frac{y}{sc.} + \sinh q_n \sin q_n \frac{y}{sc.}}{\sqrt{2}\sin q_n \sinh q_n} \qquad \text{(AI-15a)}$$

$$= \frac{\sin q_n \sinh q_n \frac{y}{sc.} + \sinh q_n \sin q_n \frac{y}{sc.}}{\sqrt{\sinh^2 q_n - \sin^2 q_n}} \qquad (n>1,\ odd) \qquad \text{(AI-15b)}$$

$$+ (-1)^{\frac{n-1}{2}} \frac{\cos \beta_n}{2} \left(e^{-q_n(1-\frac{y}{sc.})} - e^{-q_n(1+\frac{y}{sc.})} \right) \Big] \qquad \text{(AI-15c)}$$

Equations (AI-14, 15 a,b) are convenient for evaluating functions of the modes while equations (AI-14, 15c) are useful for numerical computation of the modes themselves.

The solutions for $n = 0, 1$ correspond to the so-called rigid modes and are given by

$$g_0(y) = \frac{1}{\sqrt{2}}, \qquad \text{(AI-16)}$$

$$g_1(y) = \sqrt{\frac{3}{2}} \frac{y}{sc.} \qquad \text{(AI-17)}$$

3. Simply Supported Bar of Length L :

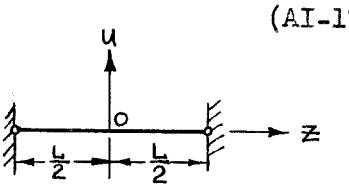

The boundary conditions are

$$u = \frac{d^2u}{dz^2} = 0 \qquad at \qquad z = \pm \frac{L}{2}. \qquad \text{(AI-18)}$$

It can be verified directly that these conditions are satisfied by the normalized solutions

$$h_m\left(\frac{z}{L}\right) = \sqrt{2}\cos m\pi\frac{z}{L} = \sqrt{2}\cos r_m \frac{z}{L}, \quad m \text{ odd}$$

$$= \sqrt{2}\sin m\pi\frac{z}{L} = \sqrt{2}\sin r_m \frac{z}{L}, \quad m \text{ even} \qquad \text{(AI-19)}$$

which indicates that the characteristic values are

$$r_m = m\pi. \qquad \text{(AI-20)}$$

C. Evaluation of Defined Functions of the Modes

Looking at equation (AI-1), we see that any order derivative of u also satisfies the differential equation. (If we let primes indicate differentiation with respect to $m\frac{x}{l}$, $u'''' = u$; hence, for example, $u^{VI} = u''$ which is the same as $(u'')'''' = (u'')$.) Thus, any order derivative of u whose boundary conditions are physically possible is the vibration mode for a bar with these same boundary conditions. For example, at a clamped end, we have $u = u' = 0$ which is the same as $u'''' = u^{V} = 0$ or $(u'')'' = (u'')''' = 0$ and at a free end, $u'' = u''' = 0$ or $(u'') = (u'')' = 0$. Thus the second derivative of say the third mode of a "clamped-free" bar is the third mode of a "free-clamped" bar. The orthogonality property for <u>any</u> solution of the differential equation which satisfies physically possible boundary conditions is established by the general Sturm-Liouville theorem of eigenfunctions. Consequently, we may deduce the validity of equation (I-14) and the first two parts of equation (II-9). (It should be noted in regard to equation (II-9) that the boundary conditions $u' = u''' = 0$ are physically possible although experimentally impractical.)

$\tau_{mn} = 0$ for $m \neq n$ follows from the fact that, except for a constant, $h_m\left(\frac{\xi}{L}\right) = h_m''\left(\frac{\xi}{L}\right)$. $\varphi_{mn} = \omega_{mn} = 0$ for any m,n results from the integration of the product of an odd and even function over an interval whose center is the origin, or from orthogonality.

The values of the remaining functions in equation (II-8) are

$$\Delta_{mm} = r_m^4 = m^4\pi^4 \qquad \text{(AI-21)}$$

$$\varepsilon_{mm} = r_m^2 = m^2\pi^2 \qquad \text{(AI-22)}$$

$$\tau_{mm} = -r_m^2 = -m^2\pi^2. \qquad \text{(AI-23)}$$

The evaluation of the functions in equation (I-13) is typified by the derivation for ψ_{mn} which follows:

From equation (AI-1):

$$f_m^{IV} = p_m^4 f_m \qquad \left(\text{where } f_m' = \frac{df_m}{d\left(\frac{\xi}{L}\right)}, \text{ etc.}\right)$$

$$\therefore \begin{cases} f_n^{V} = p_n^4 f_n' \\ f_m^{VI} = p_m^4 f_m'' \end{cases}$$

Rewriting:

$$p_m^4 f_m'' f_n' = f_n' f_m^{VI}$$

$$p_n^4 f_n' f_m'' = f_m'' f_n^{V}$$

Subtracting and integrating:

$$(p_m^4 - p_n^4)\int_0^1 f_m'' f_n' \, d\left(\frac{\xi}{L}\right) \equiv (p_m^4 - p_n^4)\psi_{mn} = \int_0^1 \left(f_n' f_m^{VI} - f_m'' f_n^{V}\right) d\left(\frac{\xi}{L}\right)$$

Integrating by parts:

$$(p_m^4 - p_n^4)\psi_{mn} = \left[f_n' f_m^{V} - f_m'' f_n^{IV}\right]_0^1 - \left[f_n'' f_m^{IV} - f_m''' f_n''\right]_0^1 + \int_0^1 \underbrace{\left(f_n''' f_m^{IV} - f_m^{IV} f_n'''\right)}_{0} d\left(\frac{\xi}{L}\right)$$

Recalling that

$$f_m^{IV} = p_m^4 f_m,$$

$$f_m^{V} = p_m^4 f_m'$$

$$f_m = f_m' = 0 \quad \text{at} \quad \frac{\xi}{L} = 0$$

$$f_m'' = f_m''' = 0 \quad \text{at} \quad \frac{\xi}{L} = 1$$

$$\psi_{mn} = \frac{p_m^4 f_n'(1) f_m'(1) - f_m'''(0) f_n''(0)}{p_m^4 - p_n^4}.$$

For $m = n$, a limiting process must be used in which $m = n + \delta n$ is substituted and the limit found as δn approaches zero.

The terminal values of the functions may be substituted to give simpler expressions. They are

$$f_m(1) = (-1)^{m+1} 2 \qquad \text{(AI-24a)}$$

$$f_m'(1) = (-1)^{m+1} 2 \sigma_m p_m \qquad \text{(AI-24b)}$$

$$f_m''(0) = 2p_m^2 \tag{AI-24c}$$

$$f_m'''(0) = -2\tau_m p_m^3 ; \tag{AI-24d}$$

for n even (except n = 0):

$$g_n(1sc.) = g_n(-1sc.) = (-1)^{\frac{n}{2}}\sqrt{2} \tag{AI-24e}$$

$$g_n'(1sc.) = -g_n'(-1sc.) = (-1)^{\frac{n}{2}}\sqrt{2}\,p_n\,q_n\,sc.^{-1} \tag{AI-24f}$$

for n odd (except n = 1):

$$g_n(1sc.) = -g_n(-1sc.) = (-1)^{\frac{n-1}{2}}\sqrt{2} \tag{AI-24g}$$

$$g_n'(1sc.) = g_n'(-1sc.) = (-1)^{\frac{n-1}{2}}\sqrt{2}\,p_n\,q_n\,sc.^{-1} \tag{AI-24h}$$

The final values of the functions are

for n ≠ m:

$$\alpha_{mn} = 0 \tag{AI-25a}$$

$$\beta_{mn} = 4\,\frac{(-1)^{m+n}(\tau_n p_n p_m^4 - \tau_m p_m p_n^4) + p_m^2 p_n^2(\tau_n p_n - \tau_m p_m)}{p_m^4 - p_n^4} \tag{AI-25b}$$

$$\gamma_{mn} = \frac{4p_m^2(\tau_m p_m - \tau_n p_n)[(-1)^{m+n}p_m^2 + p_n^2]}{p_m^4 - p_n^4} \tag{AI-25c}$$

$$\psi_{mn} = \tau_m p_m \tau_n p_n \tau_{mn} \tag{AI-25d}$$

$$\tau_{mn} = \frac{4p_m^2[(-1)^{m+n}p_m^2 - p_n^2]}{p_m^4 - p_n^4} ; \tag{AI-25e}$$

for n = m:

$$\alpha_{mm} = p_m^4 \tag{AI-25f}$$

$$\beta_{mm} = 2\tau_m p_m + \tau_m^2 p_m^2 \tag{AI-25g}$$

$$\gamma_{mm} = 2\tau_m p_m - \tau_m^2 p_m^2 \tag{AI-25h}$$

$$\psi_{mm} = 2\tau_m^2 p_m^2 \tag{AI-25i}$$

$$\tau_{mm} = 2 ; \tag{AI-25j}$$

for $n \neq m$, $n \geq 2$, $m \geq 2$:

$$\varkappa_{mn} = 0 \tag{AI-26a}$$

$$\left.\begin{aligned} \lambda_{mn} &= 0 && \text{for } (m+n) \text{ odd} \\ \lambda_{mn} &= (-1)^{\frac{3m+n}{2}} 4 \frac{q_m^4 \rho_n q_n - q_n^4 \rho_m q_m}{q_m^4 - q_n^4} \text{ sc.}^{-1} && \text{for } (m+n) \text{ even} \end{aligned}\right\} \tag{AI-26b}$$

$$\left.\begin{aligned} \mu_{mn} &= 0 && \text{for } (m+n) \text{ odd} \\ \mu_{mn} &= (-1)^{\frac{3m+n}{2}} 4 q_m^4 \frac{\rho_m q_m - \rho_n q_n}{q_m^4 - q_n^4} \text{ sc.}^{-1} && \text{for } (m+n) \text{ even} \end{aligned}\right\} \tag{AI-26c}$$

$$\left.\begin{aligned} \pi_{mn} &= 0 && \text{for } (m+n) \text{ even} \\ \pi_{mn} &= \rho_m q_m \rho_n q_n \zeta_{mn} \text{ sc.}^{-2} && \text{for } (m+n) \text{ odd} \end{aligned}\right\} \tag{AI-26d}$$

$$\left.\begin{aligned} \zeta_{mn} &= 0 && \text{for } (m+n) \text{ even} \\ \zeta_{mn} &= \frac{(-1)^{\frac{m+n-1}{2}} 4 q_m^4}{q_m^4 - q_n^4} && \text{for } (m+n) \text{ odd;} \end{aligned}\right\} \tag{AI-26e}$$

for $n = m \geq 2$:

$$\varkappa_{mm} = q_m^4 \text{ sc.}^{-3} \tag{AI-26f}$$

$$\lambda_{mm} = (\rho_m^2 q_m^2 + 3\rho_m q_m) \text{ sc.}^{-1} \tag{AI-26g}$$

$$\mu_{mm} = (\rho_m q_m - \rho_m^2 q_m^2) \text{ sc.}^{-1} \tag{AI-26h}$$

$$\pi_{mm} = 0 \tag{AI-26i}$$

$$\zeta_{mm} = 0. \tag{AI-26j}$$

If n or m = 0 or 1, a "rigid" mode is involved, and equations (AI-26), which were based on equation (AI-1), are not applicable. With the aid of the expressions presented in Appendix II, the following formulas for these cases can be verified.

$$\varkappa_{mn} = 0 \qquad \text{for } m = 0, 1 \text{ or } n = 0,1. \tag{AI-27a}$$

$$\lambda_{mn} = 0 \qquad \text{for } m = 0 \text{ or } n = 0$$

$$\lambda_{11} = 3\,sc.^{-1}$$

for $m \geq 2$:

$$\lambda_{m1} = \lambda_{1m} = (-1)^{\frac{m-1}{2}} 2\sqrt{3}\; sc.^{-1} \qquad \text{for } m \text{ odd}$$

$$= 0 \qquad \text{for } m \text{ even.}$$

(AI-27b)

$$\mu_{mn} = 0 \qquad \text{for } m = 0,1;$$

for $m \geq 2$:

$$\mu_{m0} = (-1)^{\frac{m}{2}} 2\rho_m q_m\; sc.^{-1} \qquad \text{for } m \text{ even}$$

$$= 0 \qquad \text{for } m \text{ odd}$$

$$\mu_{m1} = (-1)^{\frac{m-1}{2}} 2\sqrt{3}\,(\rho_m q_m - 1)\, sc.^{-1} \qquad \text{for } m \text{ odd}$$

$$= 0 \qquad \text{for } m \text{ even.}$$

(AI-27c)

$$\pi_{mn} = 0 \qquad \text{for } m = 0,1, \text{ or } n = 0;$$

for $m \geq 2$:

$$\pi_{m1} = (-1)^{\frac{m}{2}} 2\sqrt{3}\rho_m q_m\; sc.^{-2} \qquad \text{for } m \text{ even}$$

$$= 0 \qquad \text{for } m \text{ odd.}$$

(AI-27d)

$$\varsigma_{mn} = 0 \qquad \text{for } m = 0,1 \text{ (except } m,n = 1,0)$$

$$\varsigma_{10} = \sqrt{3}$$

for $m \geq 2$:

$$\varsigma_{m0} = (-1)^{\frac{m-1}{2}} 2 \qquad \text{for } m \text{ odd}$$

$$= 0 \qquad \text{for } m \text{ even}$$

$$\varsigma_{m1} = (-1)^{\frac{m}{2}} 2\sqrt{3} \qquad \text{for } m \text{ even}$$

$$= 0 \qquad \text{for } m \text{ odd.}$$

(AI-27e)

APPENDIX II - FORMULAE FOR SOME INTEGRALS INVOLVING $f_m\left(\frac{\xi}{L}\right)$ AND $g_n(\eta)$

The following integrals occur frequently in the evaluation of the constant terms, m_{mn}, whether or not an approximate deflection function, w_o, is used. They are presented without proof, but their derivations are not in general difficult. The latter can be accomplished by one or a combination of the following methods.

a. Direct substitution of the functions, followed by integration.

b. Integration in symbolic notation, e.g.

$$\int_a^b f'(x)\,dx = f(x)\Big|_a^b = f(b) - f(a).$$

c. Integration by parts followed by a. and/or b.

d. Substituting a lower derivative of a vibration mode of a bar with complementary boundary conditions, based on the first paragraph of Section AI-C, e.g. $f_m''\left(\frac{\xi}{L}\right) = (-1)^{m+1} p_m^2 f_m\left(1-\frac{\xi}{L}\right)$.

In these equations, the primes indicate differentiation of $f_m\left(\frac{\xi}{L}\right)$ with respect to $\frac{\xi}{L}$ and of $g_n(\eta)$ with respect to η.

$$\int_0^1 f_m\left(\frac{\xi}{L}\right) d\left(\frac{\xi}{L}\right) = 2\,\frac{\sigma_m}{p_m} \tag{AII-1}$$

$$\int_0^1 f_m'\left(\frac{\xi}{L}\right) d\left(\frac{\xi}{L}\right) = (-1)^{m+1} 2 \tag{AII-2}$$

$$\int_0^1 f_m''\left(\frac{\xi}{L}\right) d\left(\frac{\xi}{L}\right) = (-1)^{m+1} 2\sigma_m p_m \tag{AII-3}$$

$$\int_0^1 \left(\frac{\xi}{L}\right) f_m\left(\frac{\xi}{L}\right) d\left(\frac{\xi}{L}\right) = \frac{2}{p_m^2} \tag{AII-4}$$

$$\int_0^1 \left(\frac{\xi}{L}\right) f_m'\left(\frac{\xi}{L}\right) d\left(\frac{\xi}{L}\right) = 2\left[(-1)^{m+1} - \frac{\sigma_m}{p_m}\right] \tag{AII-5}$$

$$\int_0^1 \left(\frac{\xi}{L}\right) f_m''\left(\frac{\xi}{L}\right) d\left(\frac{\xi}{L}\right) = (-1)^{m+1} 2\left(\sigma_m p_m - 1\right) \tag{AII-6}$$

$$\int_{-1sc.}^{1sc.} g_n(\eta)\,d\eta = \begin{cases} 0 & \text{if } n = 0 \\ \sqrt{2}\ sc. & \text{if } n \neq 0 \end{cases} \qquad \text{(AII-7)}$$

$$\int_{-1sc.}^{1sc.} g_n'(\eta)\,d\eta = \begin{cases} (-1)^{\frac{n-1}{2}} 2\sqrt{2} & \text{if n is odd} \\ 0 & \text{if n is even} \end{cases} \qquad \text{(AII-8)}$$

$$\int_{-1sc.}^{1sc.} g_n''(\eta)\,d\eta = \begin{cases} (-1)^{\frac{n}{2}} 2\sqrt{2}\,\rho_n q_n\ sc.^{-1} & \text{if n is even} \\ 0 & \text{if n is odd} \end{cases} \qquad \text{(AII-9)}$$

$$\int_{-1sc.}^{1sc.} \eta\, g_n(\eta)\,d\eta = \begin{cases} \sqrt{\frac{2}{3}}\ sc.^2 & \text{if } n = 1 \\ 0 & \text{if } n \neq 1 \end{cases} \qquad \text{(AII-10)}$$

$$\int_{-1sc.}^{1sc.} \eta\, g_n'(\eta)\,d\eta = \begin{cases} 0 & \text{if } \begin{cases} n \text{ is odd} \\ n = 0 \end{cases} \\ (-1)^{\frac{n}{2}} 2\sqrt{2}\ sc. & \text{if n is even and } > 0 \end{cases} \qquad \text{(AII-11)}$$

$$\int_{-1sc.}^{1sc.} \eta\, g_n''(\eta)\,d\eta = \begin{cases} (-1)^{\frac{n-1}{2}} 2\sqrt{2}\,(\rho_n q_n - 1) & \text{if n is odd} \\ 0 & \text{if n is even} \end{cases} \qquad \text{(AII-12)}$$

Higher order expressions of the same type may also be evaluated if necessary.

APPENDIX III - FORMULAE FOR THE CONSTANT TERMS OF THE SIMULTANEOUS EQUATIONS FOR SOME LOADING CONDITIONS

If no approximate deflection function is used (i.e. $W_o = 0$), the constant term of the typical simultaneous equation is

$$m_{mn} = -\frac{L^2 \cos^3\theta}{D} \frac{\partial V_o}{\partial a_{mn}} . \qquad \text{(AIII-1)}$$

The following formulae apply when q is the uniform surface loading, and Q, k, F_Q, and F_k are as defined in Figure 6.

$$q: \quad m_{mn} = \frac{2\sqrt{2}\, q L^{5/2} \cos^4\theta}{D} \frac{\sigma_m}{p_m} \text{ sc.} \quad \text{if } n = 0$$
$$= 0 \quad \text{if } n \neq 0 \qquad \text{(AIII-2)}$$

$$Q: \quad m_{mn} = \frac{(-1)^{m+1} 2\sqrt{2}\, Q L^{3/2} \cos^3\theta \text{ sc.}}{D} \quad \text{if } n = 0$$
$$= 0 \quad \text{if } n \neq 0 \qquad \text{(AIII-3)}$$

$$k: \quad m_{mn} = \frac{(-1)^{m+1} 2\sqrt{\tfrac{2}{3}}\, k L^{3/2} \cos^3\theta \text{ sc.}^2}{} \quad \text{if } n = 1$$
$$= 0 \quad \text{if } n \neq 1 \qquad \text{(AIII-4)}$$

$$F_Q: \quad m_{mn} = \frac{F_Q L^{3/2} \cos^3\theta\, f_m\left(\frac{\xi_i}{L}\right) \sum_{i=1}^{10} g_n(\eta_i)}{D} \qquad \text{(AIII-5)}$$

$$F_k: \quad m_{mn} = \frac{10 F_k L^{3/2} \cos^3\theta\, f_m\left(\frac{\xi_i}{L}\right) \sum_{i=1}^{10} \eta_i\, g_n(\eta_i)}{D \text{ sc.}} \qquad \text{(AIII-6)}$$

LIST OF FIGURES

LIST OF FIGURES (Continued)

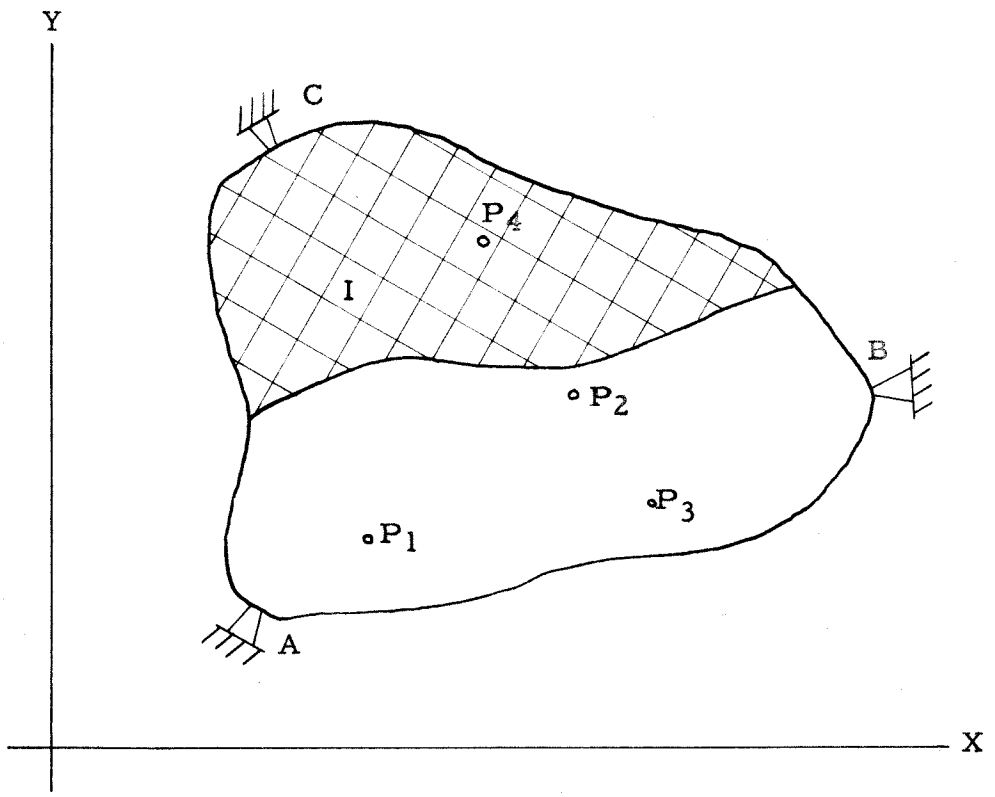

UNIFORMLY LOADED OVER REGION I.
CONCENTRATED LATERAL LOADS P_1, P_2, P_3, AND P_4, AS SHOWN.
SIMPLY SUPPORTED AT A, B, C,
THICKNESS AND MATERIAL PROPERTIES AS SPECIFIED.

FIGURE 1

ARBITRARY PLATE PROBLEM

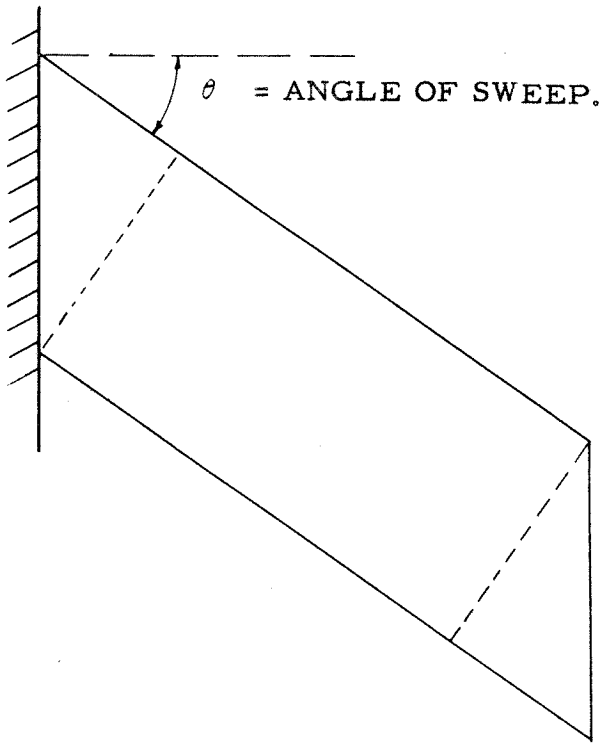

(a)

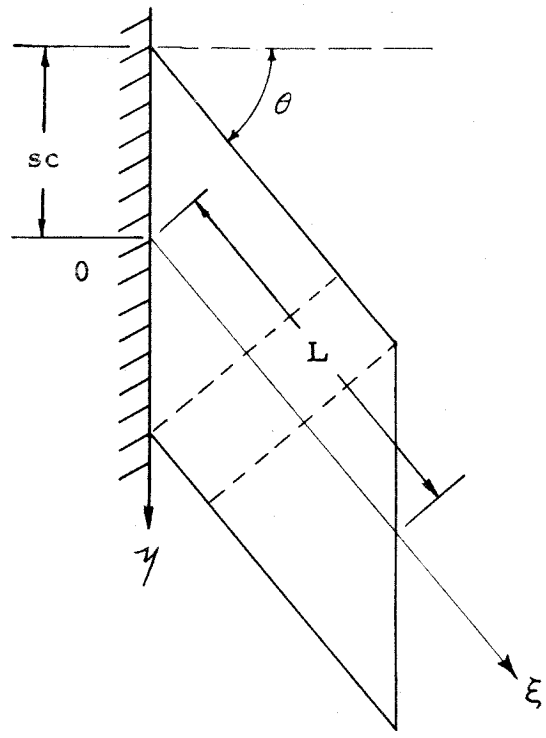

(b)

FIGURE 2

AIRCRAFT WINGS IDEALIZED TO FLAT PLATES.

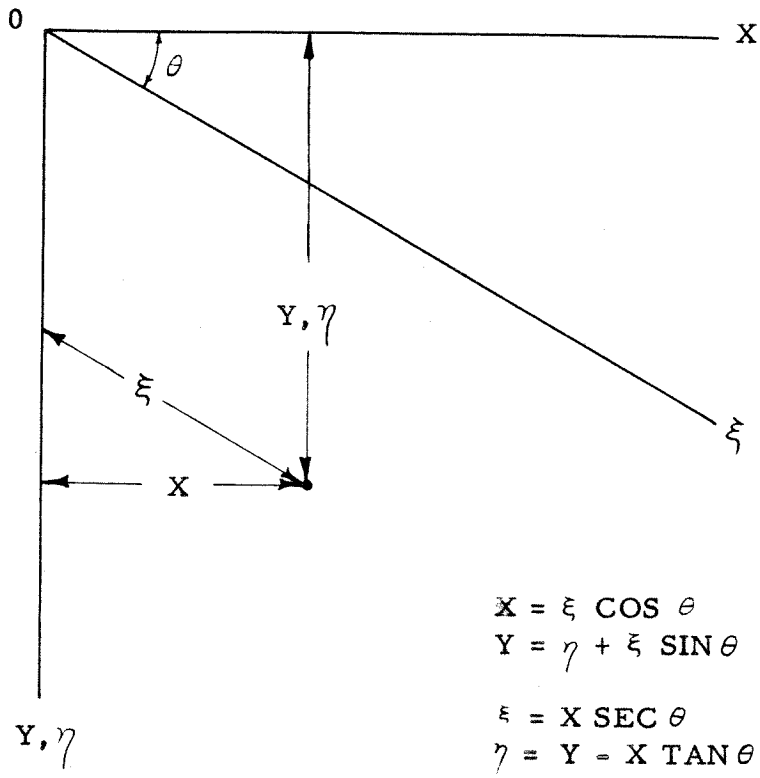

FIGURE 3

RELATION BETWEEN RECTANGULAR AND SKEW COORDINATE SYSTEMS.

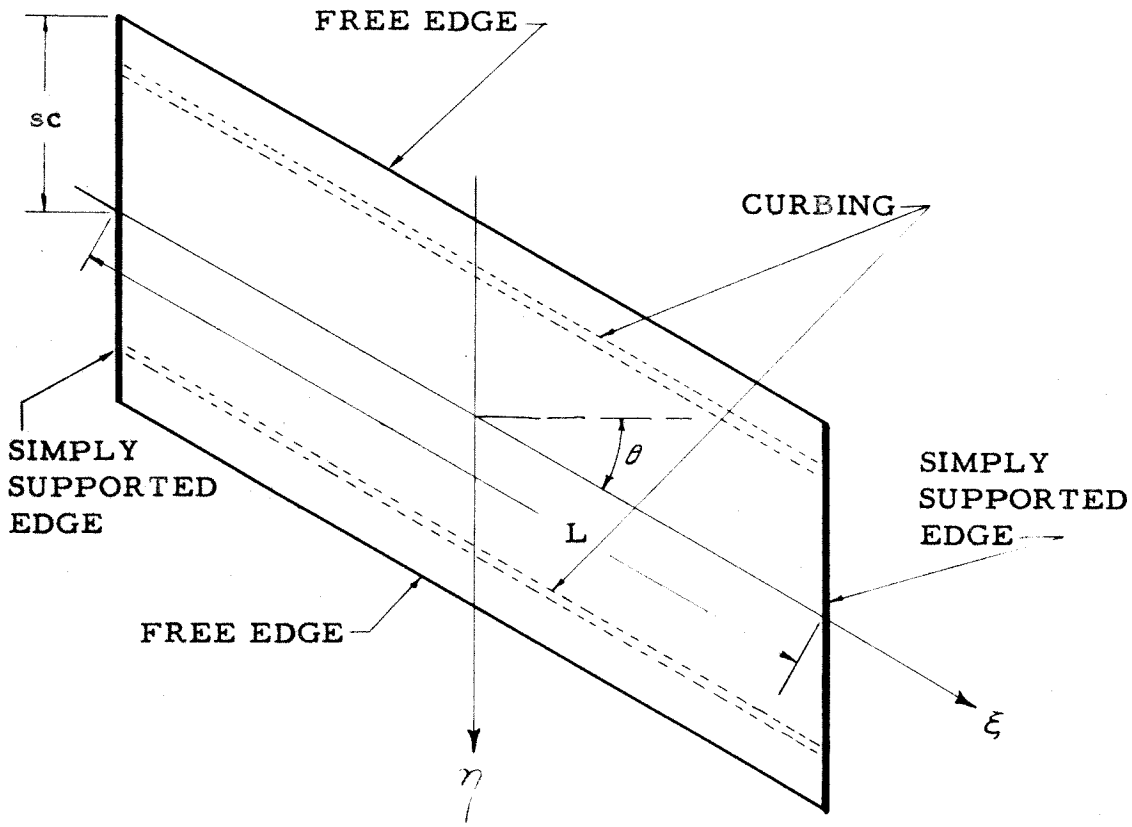

FIGURE 4

SKEW HIGHWAY BRIDGE IDEALIZED TO A
FLAT PLATE.

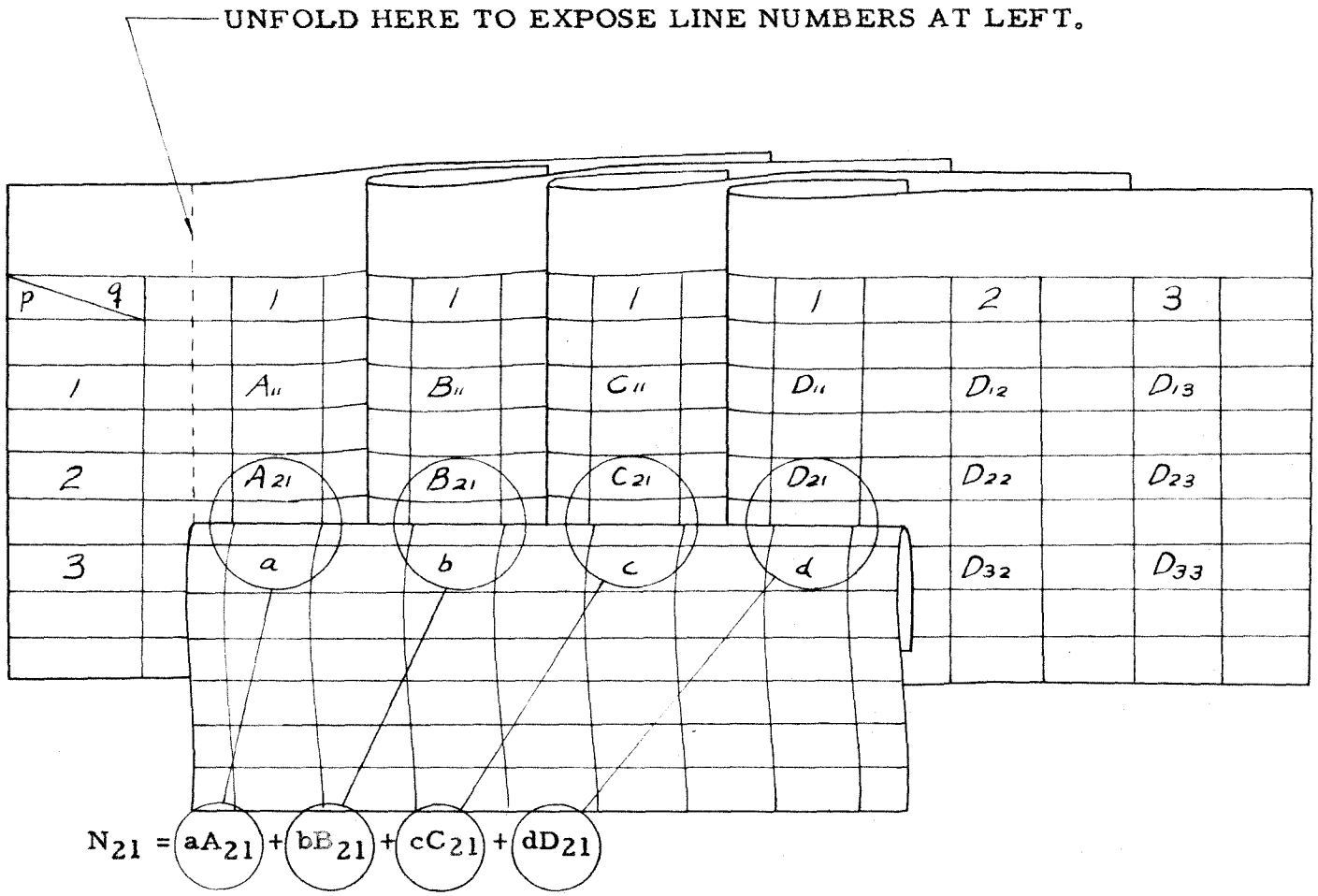

FIGURE 5

SKETCH OF ARRANGEMENT USED IN LINEAR COMBINATION OF MATRICES.

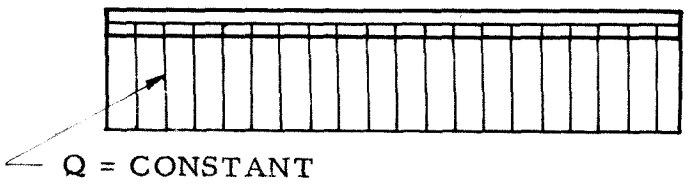

UNIFORM SHEAR

DIMENSIONS OF Q ARE $\left[FL^{-1}\right]$

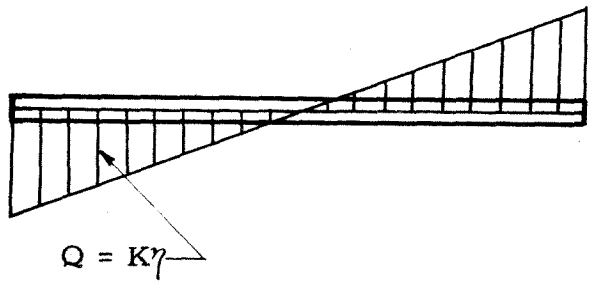

TORSION

DIMENSIONS OF K ARE $\left[FL^{-2}\right]$

(a)

CONTINUOUS LOADING

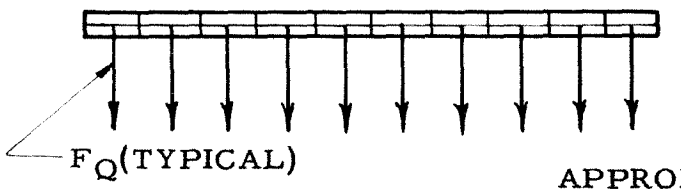

UNIFORM SHEAR

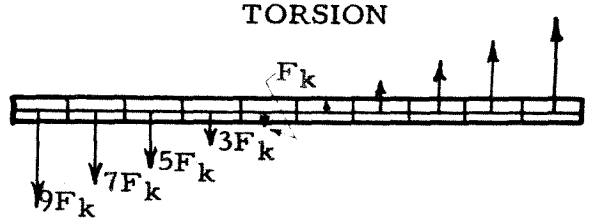

TORSION

(b)

APPROXIMATIONS TO CONTINUOUS LOADING

FIGURE 6

TYPES OF TIP LOADING

SPANWISE DEFLECTION CURVES FOR
UNIFORM SURFACE LOADING,
20° SWEEPBACK.

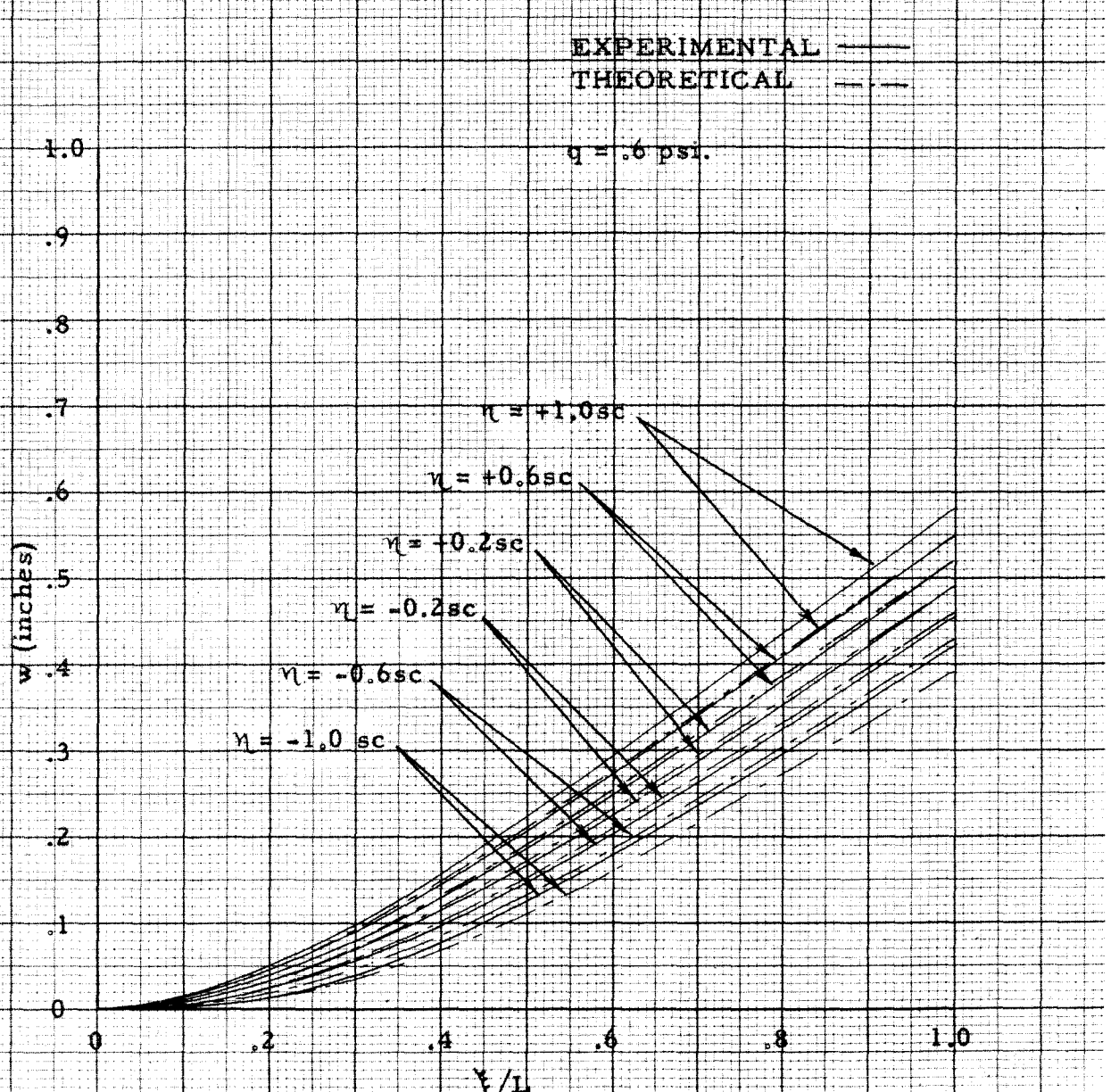

FIGURE 7

CHORDWISE DEFLECTION CURVES FOR
UNIFORM SURFACE LOADING,
20° SWEEPBACK.

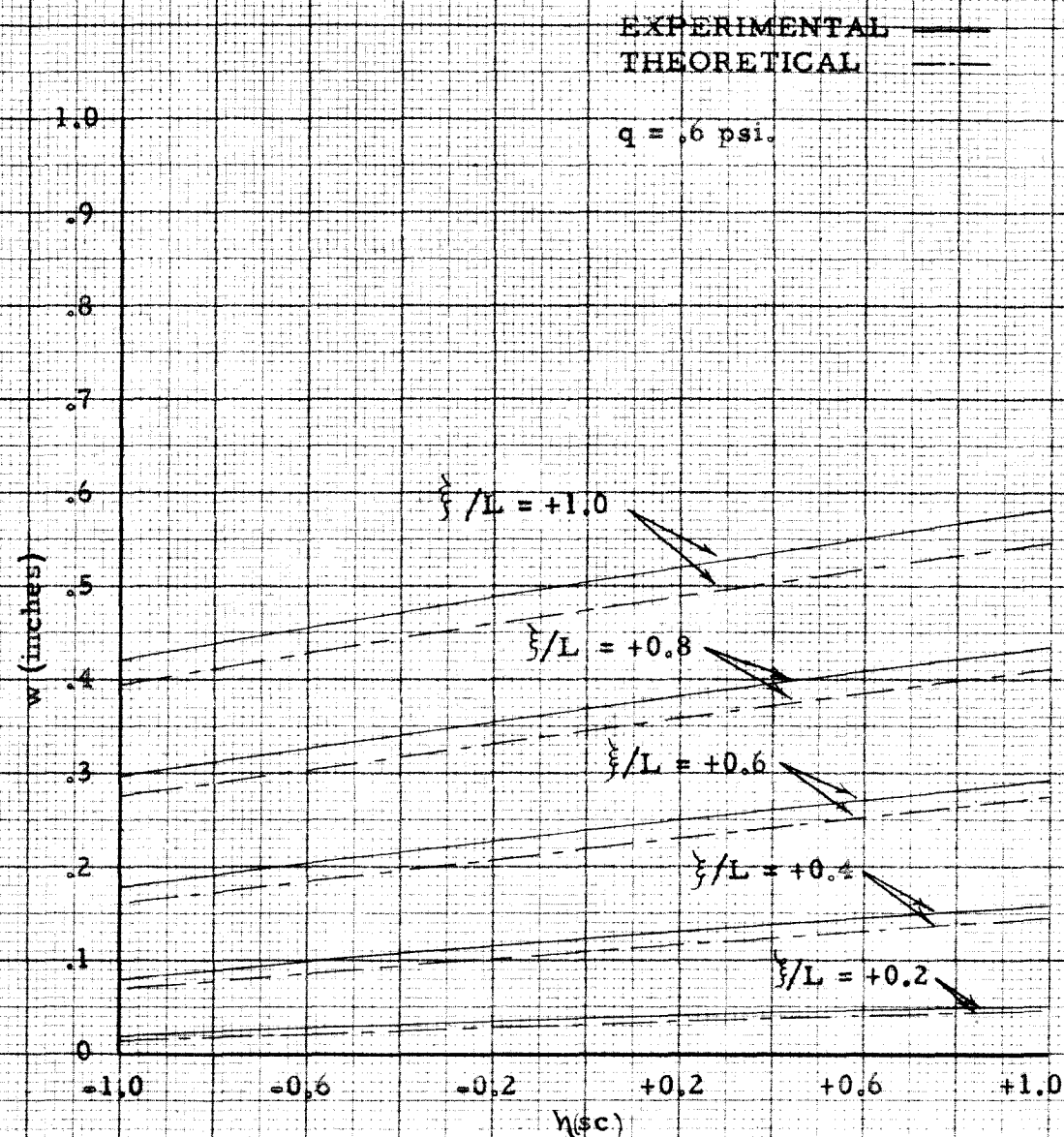

FIGURE 8

SPANWISE DEFLECTION CURVES FOR
UNIFORM TIP SHEAR,
20° SWEEPBACK.

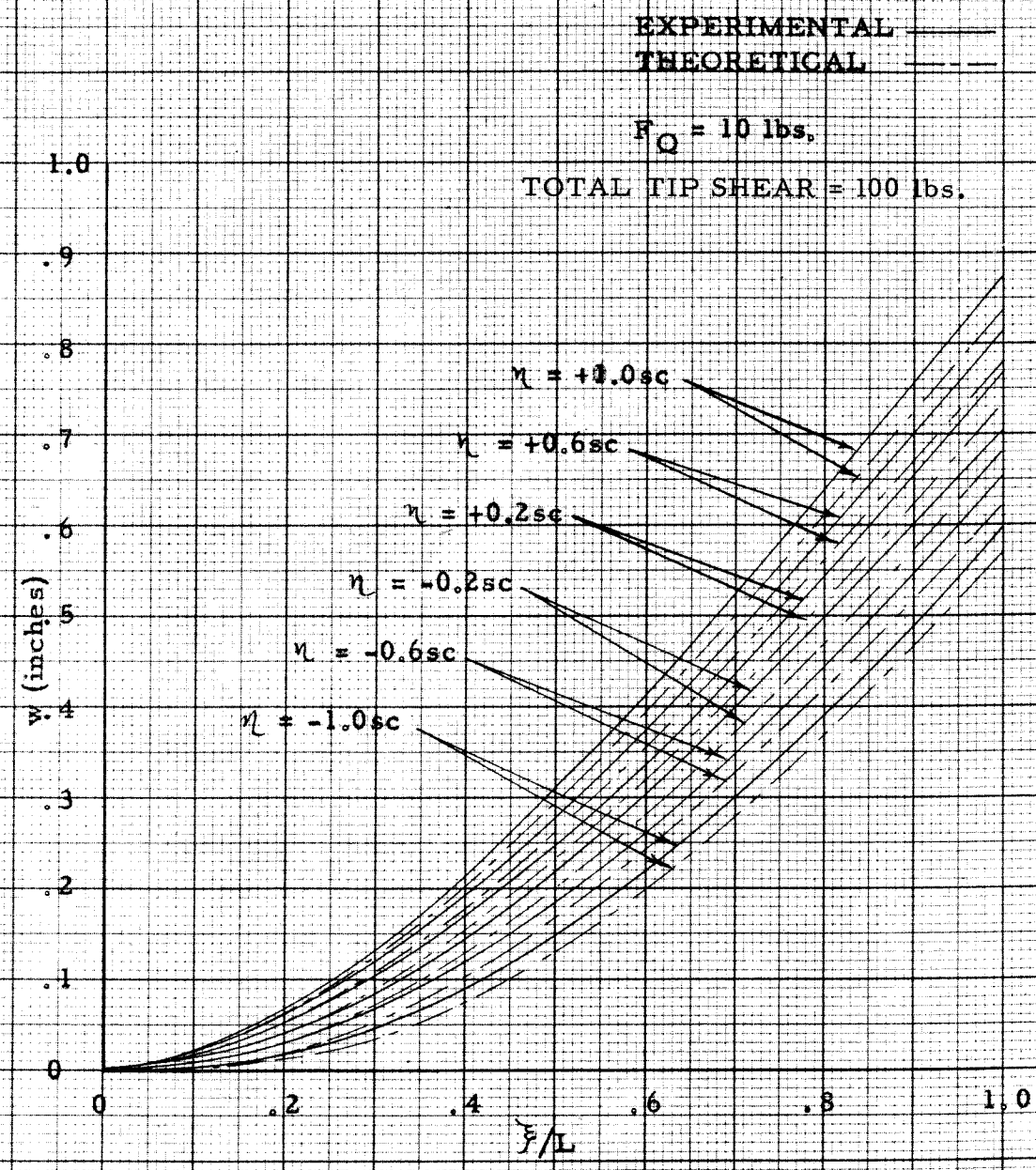

FIGURE 9

CHORDWISE DEFLECTION CURVES FOR
UNIFORM TIP SHEAR,
20° SWEEPBACK.

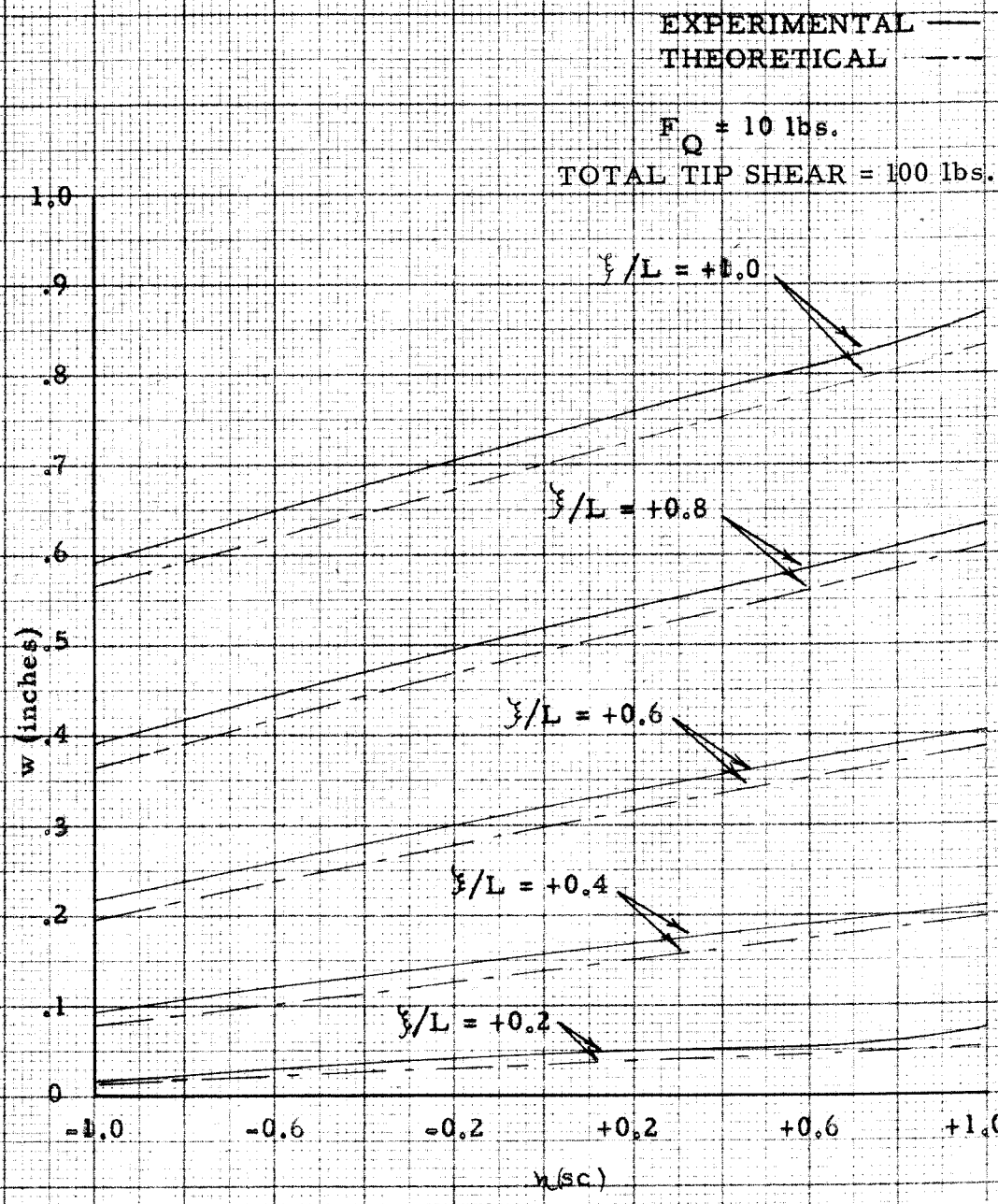

FIGURE 10

SPANWISE DEFLECTION CURVES FOR
TORSION AT TIP SECTION,
20° SWEEPBACK.

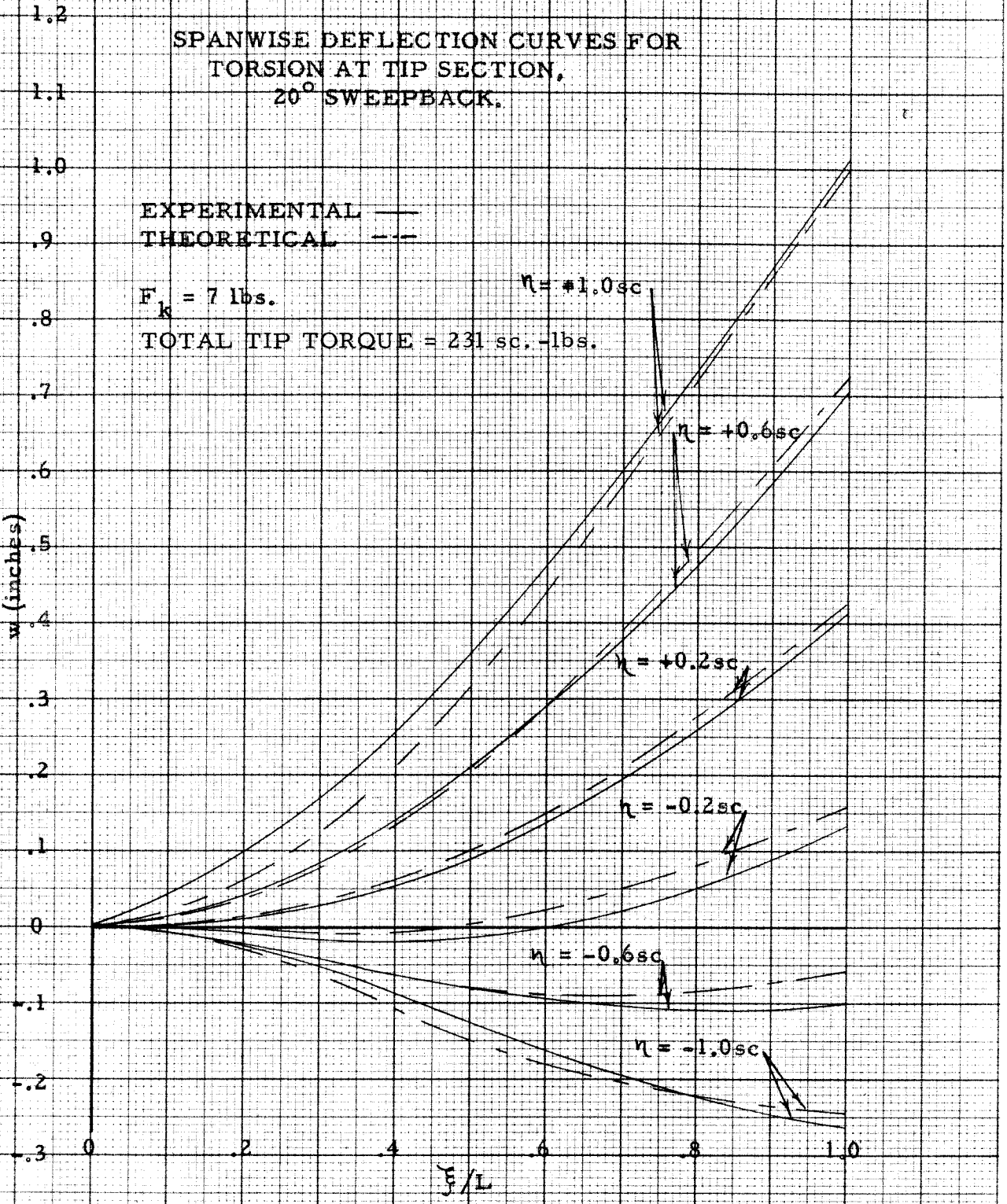

FIGURE 11

CHORDWISE DEFLECTION CURVES FOR
TORSION AT TIP SECTION,
20° SWEEPBACK.

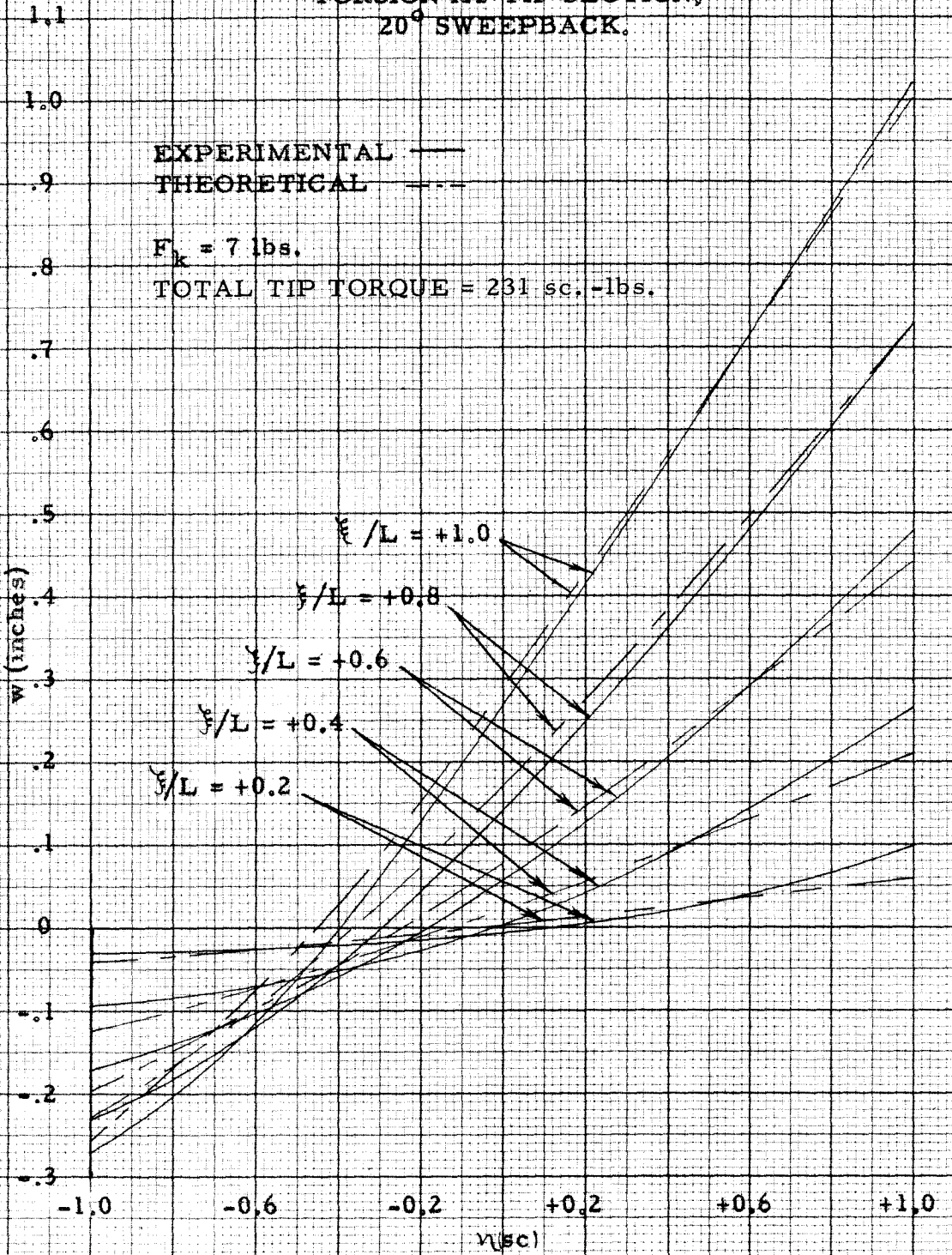

FIGURE 12

SPANWISE DEFLECTION CURVES FOR
UNIFORM SURFACE LOADING,
40° SWEEPBACK.

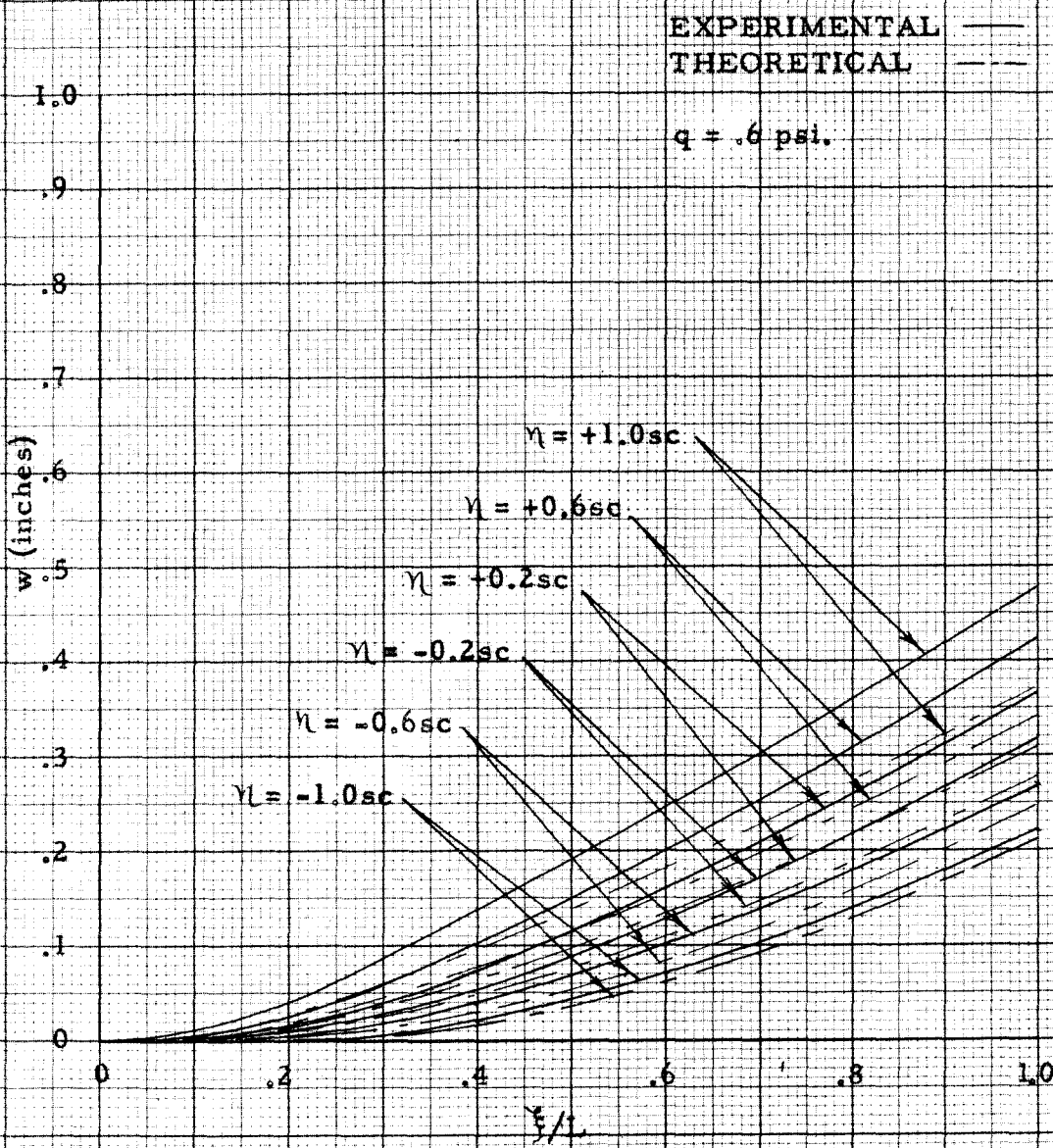

FIGURE 13

CHORDWISE DEFLECTION CURVES FOR
UNIFORM SURFACE LOADING,
40° SWEEPBACK.

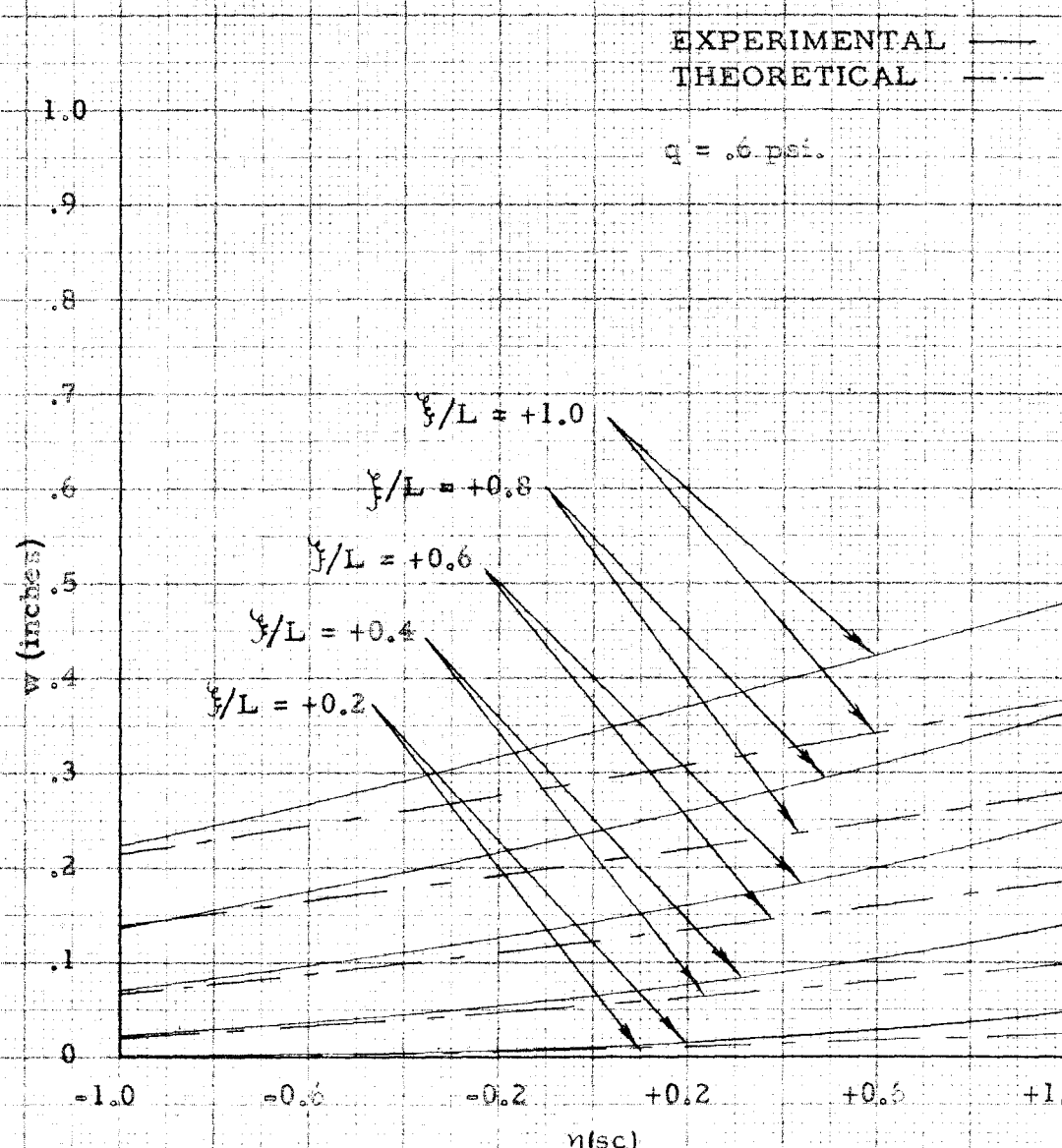

FIGURE 14

SPANWISE DEFLECTION CURVES FOR
UNIFORM TIP SHEAR,
40° SWEEPBACK.

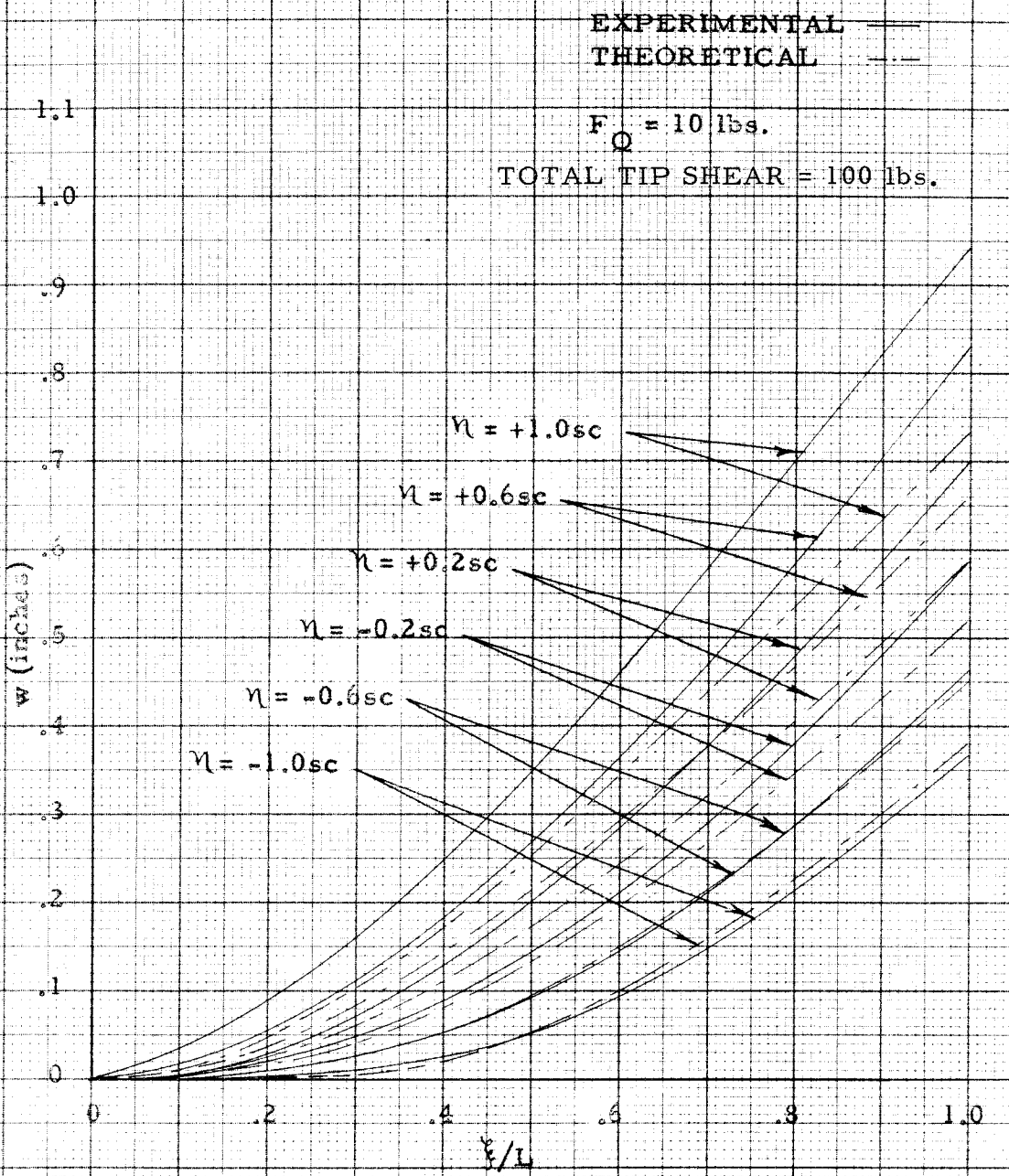

FIGURE 15

CHORDWISE DEFLECTION CURVES FOR
UNIFORM TIP SHEAR,
40° SWEEPBACK.

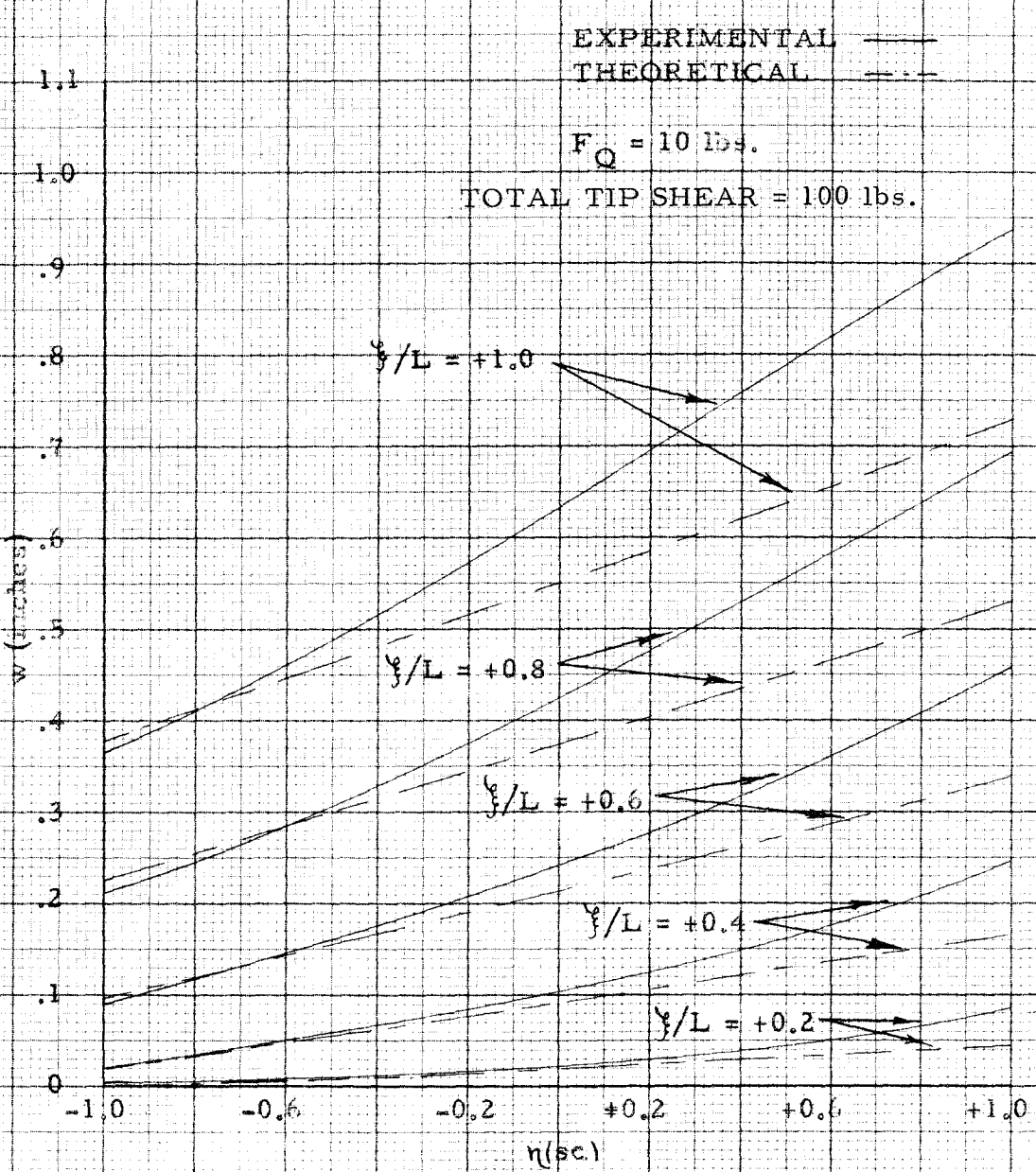

FIGURE 16

SPANWISE DEFLECTION CURVES FOR
TORSION AT TIP SECTION,
40° SWEEPBACK.

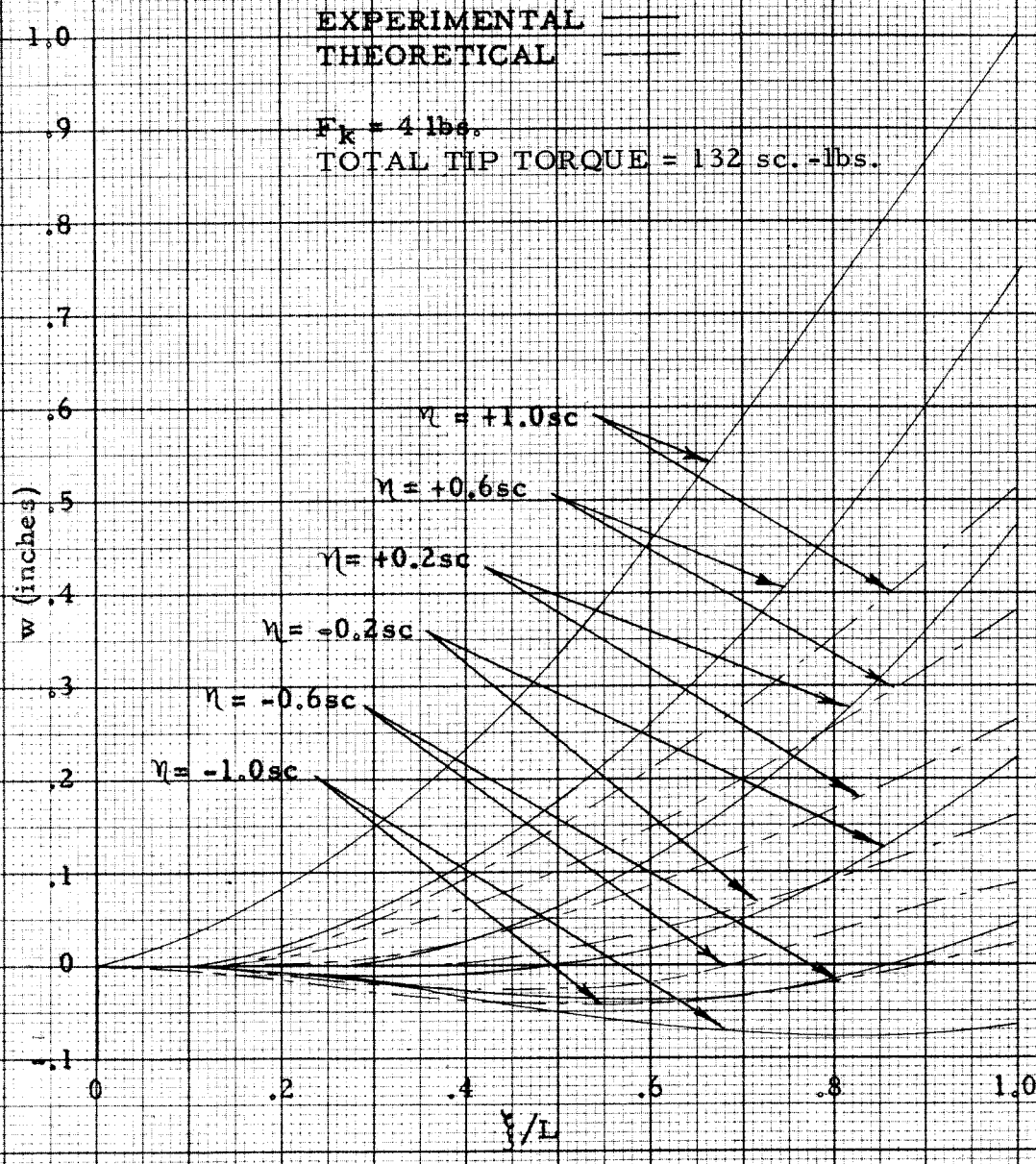

FIGURE 17

CHORDWISE DEFLECTION CURVES FOR
TORSION AT TIP SECTION,
40° SWEEPBACK.

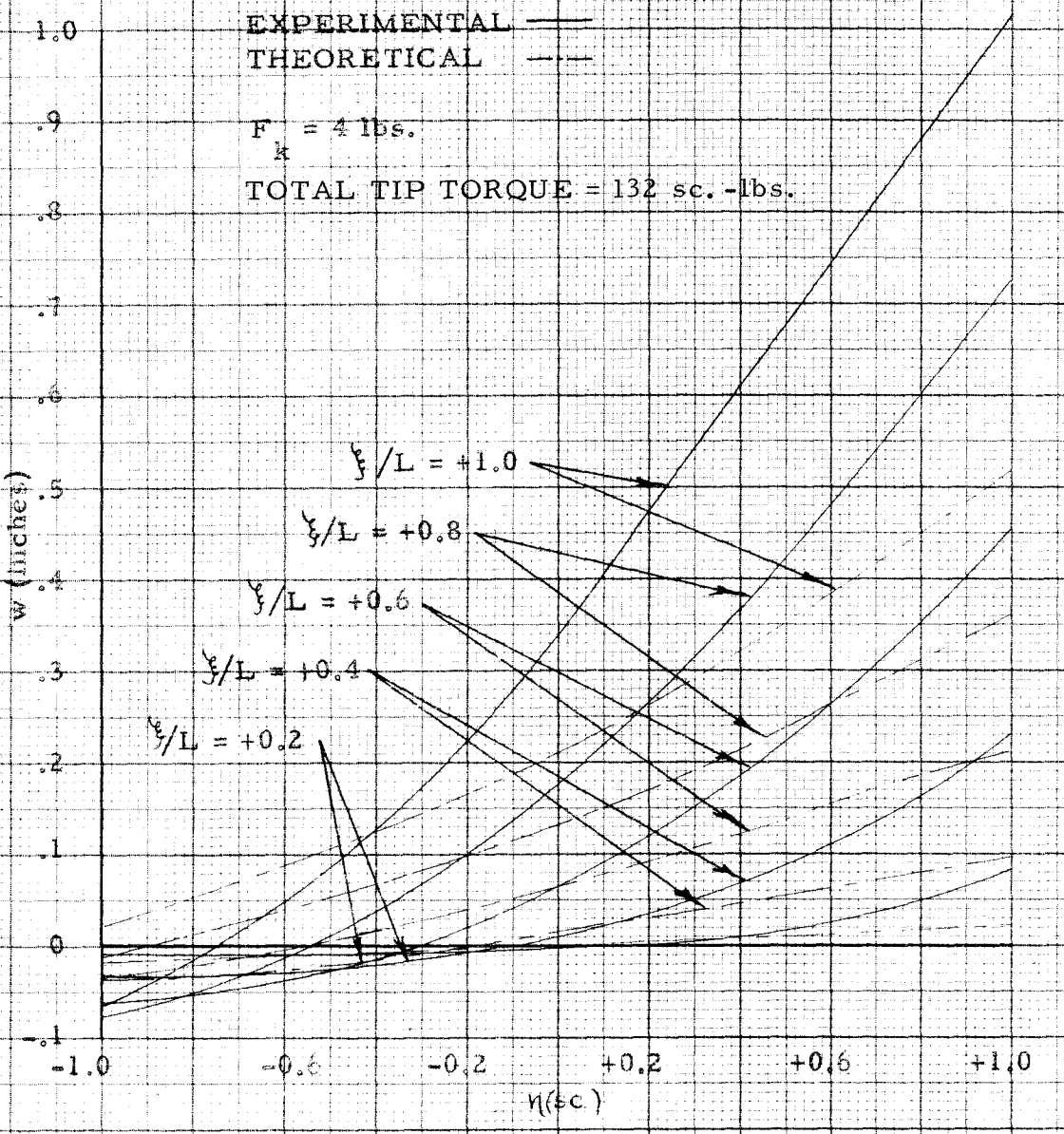

FIGURE 18

SPANWISE DEFLECTION CURVES FOR
UNIFORM SURFACE LOADING,
60° SWEEPBACK.

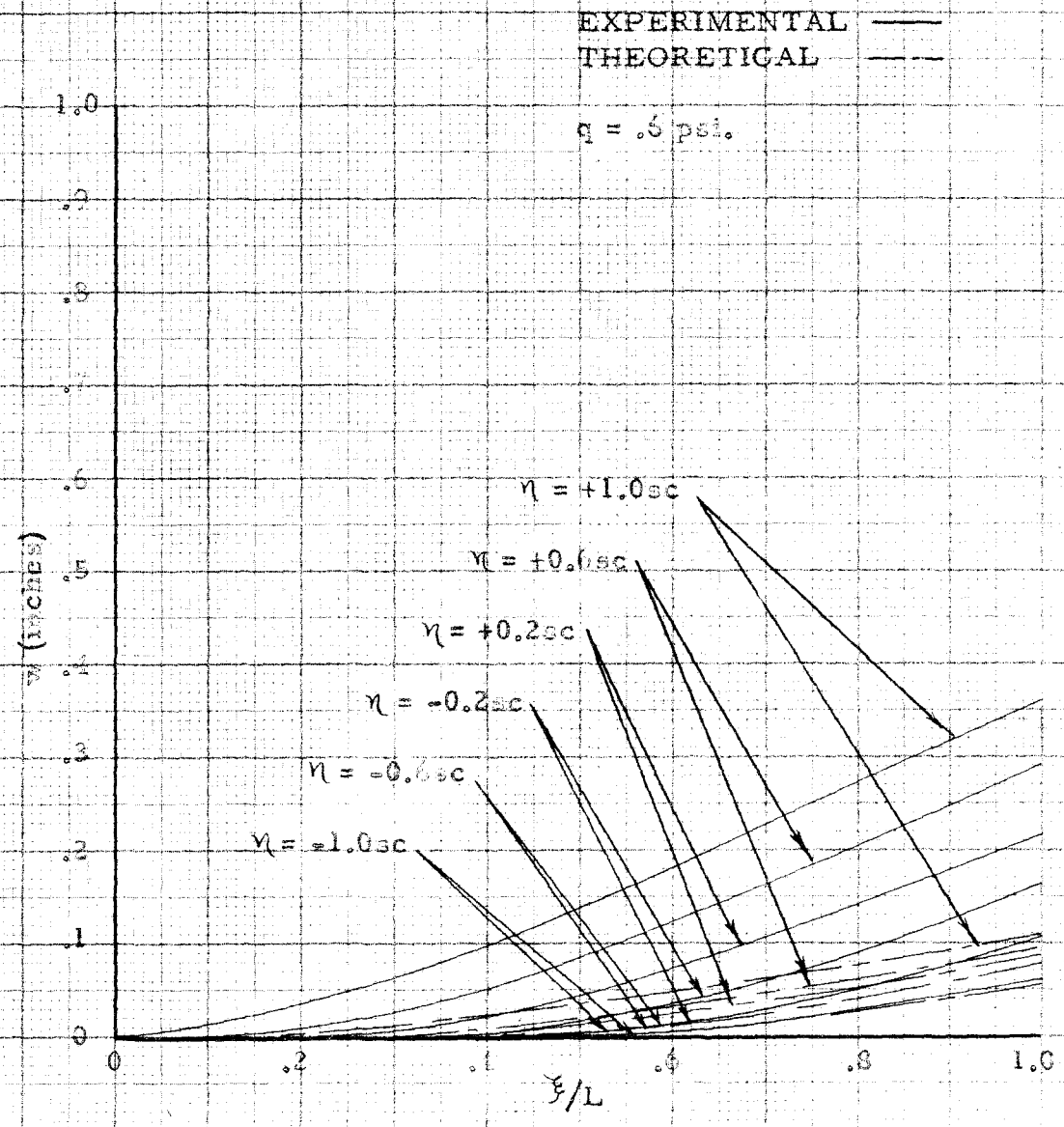

FIGURE 19

CHORDWISE DEFLECTION CURVES FOR
UNIFORM SURFACE LOADING,
60° SWEEPBACK.

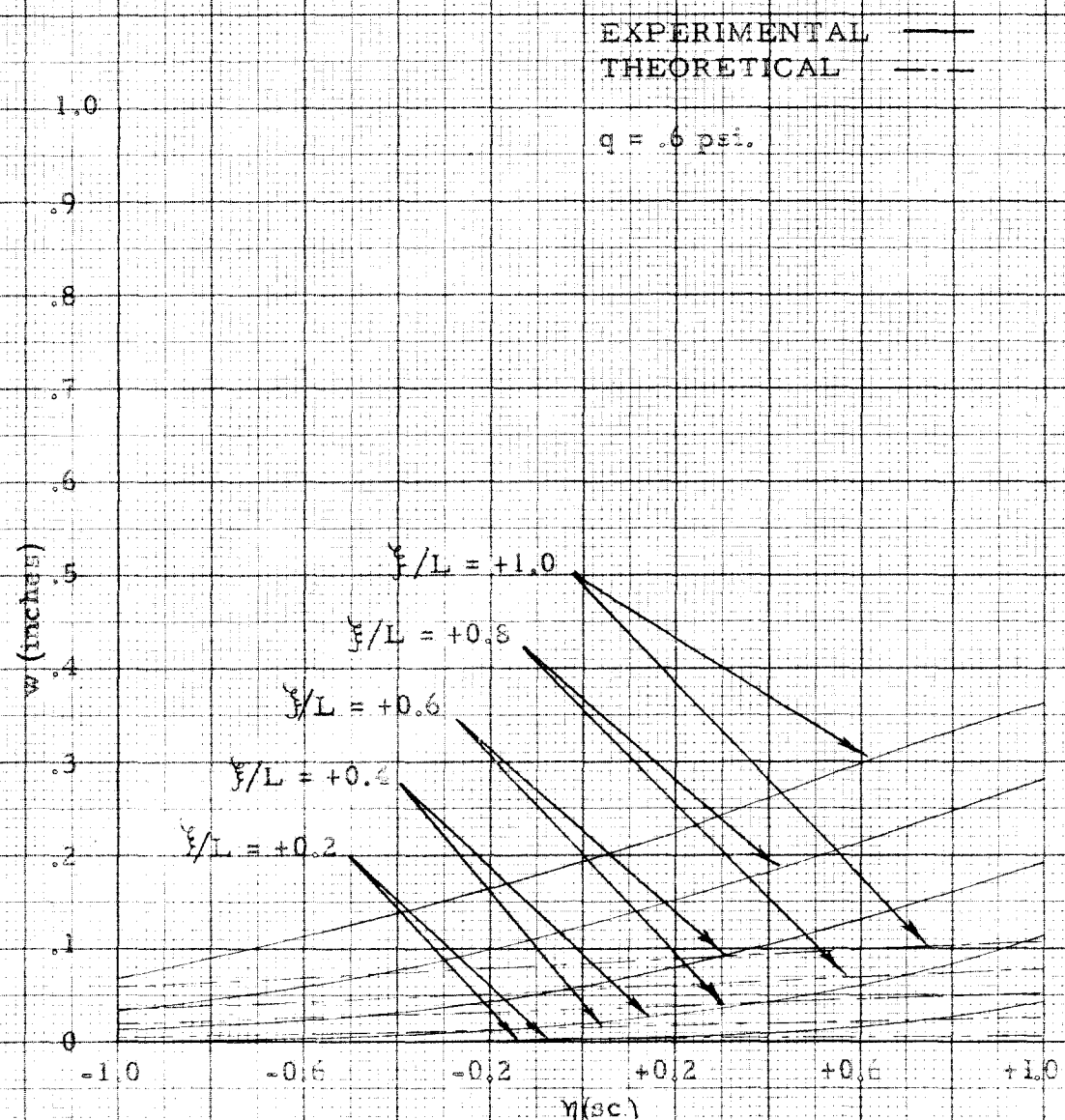

FIGURE 20

SPANWISE DEFLECTION CURVES FOR
UNIFORM TIP SHEAR,
60° SWEEPBACK.

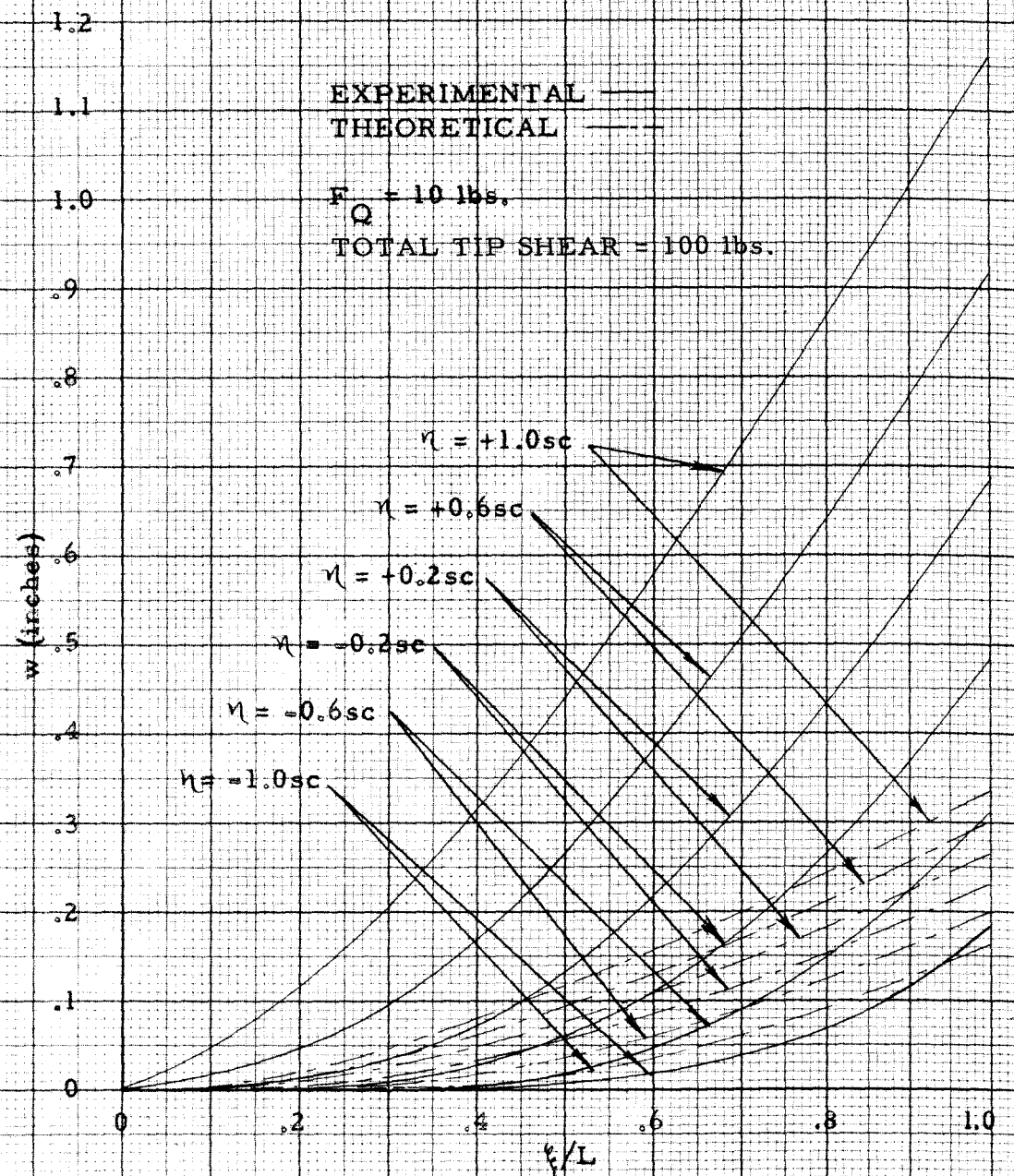

FIGURE 21

CHORDWISE DEFLECTION CURVES FOR
UNIFORM TIP SHEAR,
60° SWEEPBACK.

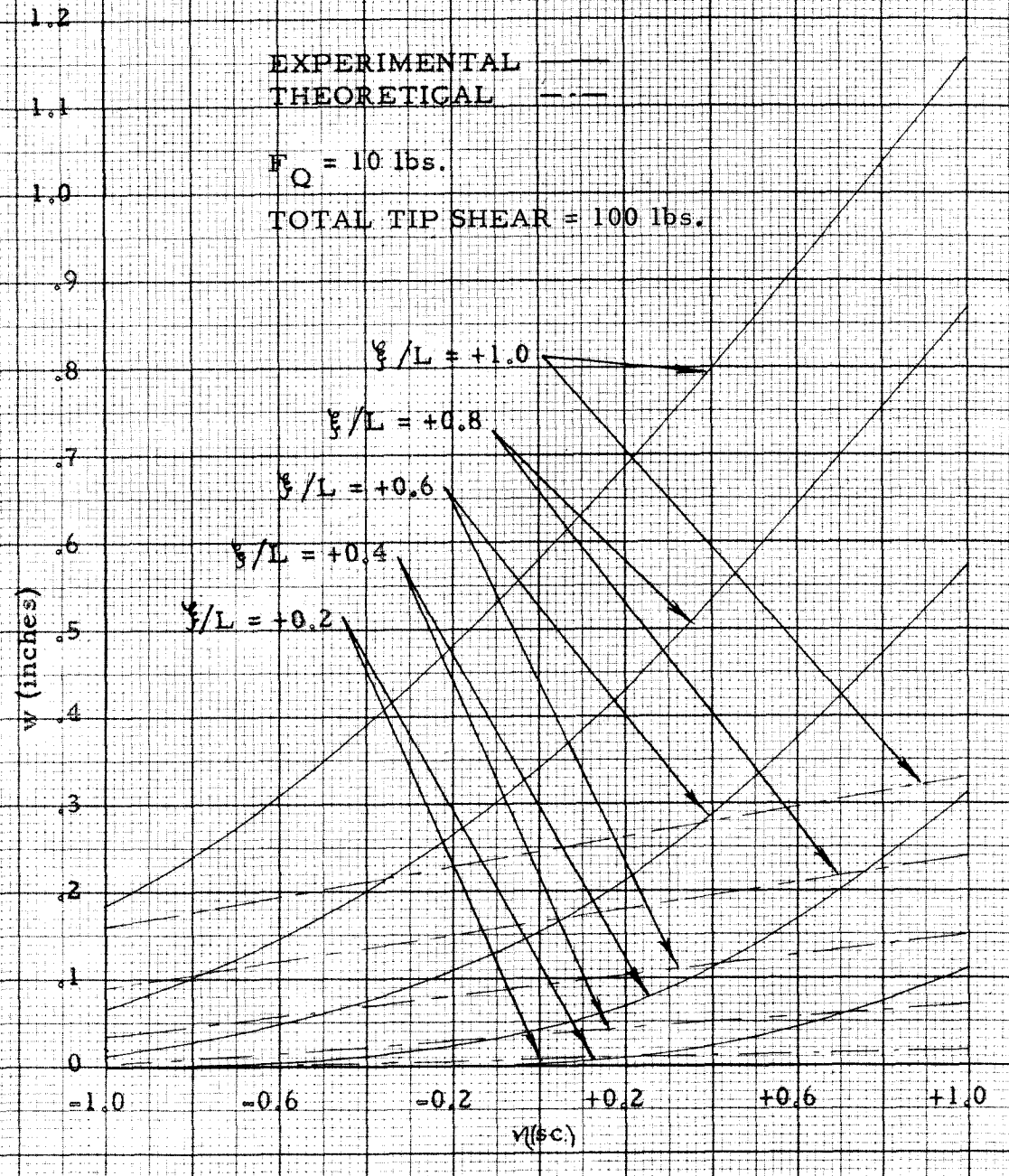

FIGURE 22

SPANWISE DEFLECTION CURVES FOR
TORSION AT TIP SECTION,
60° SWEEPBACK.

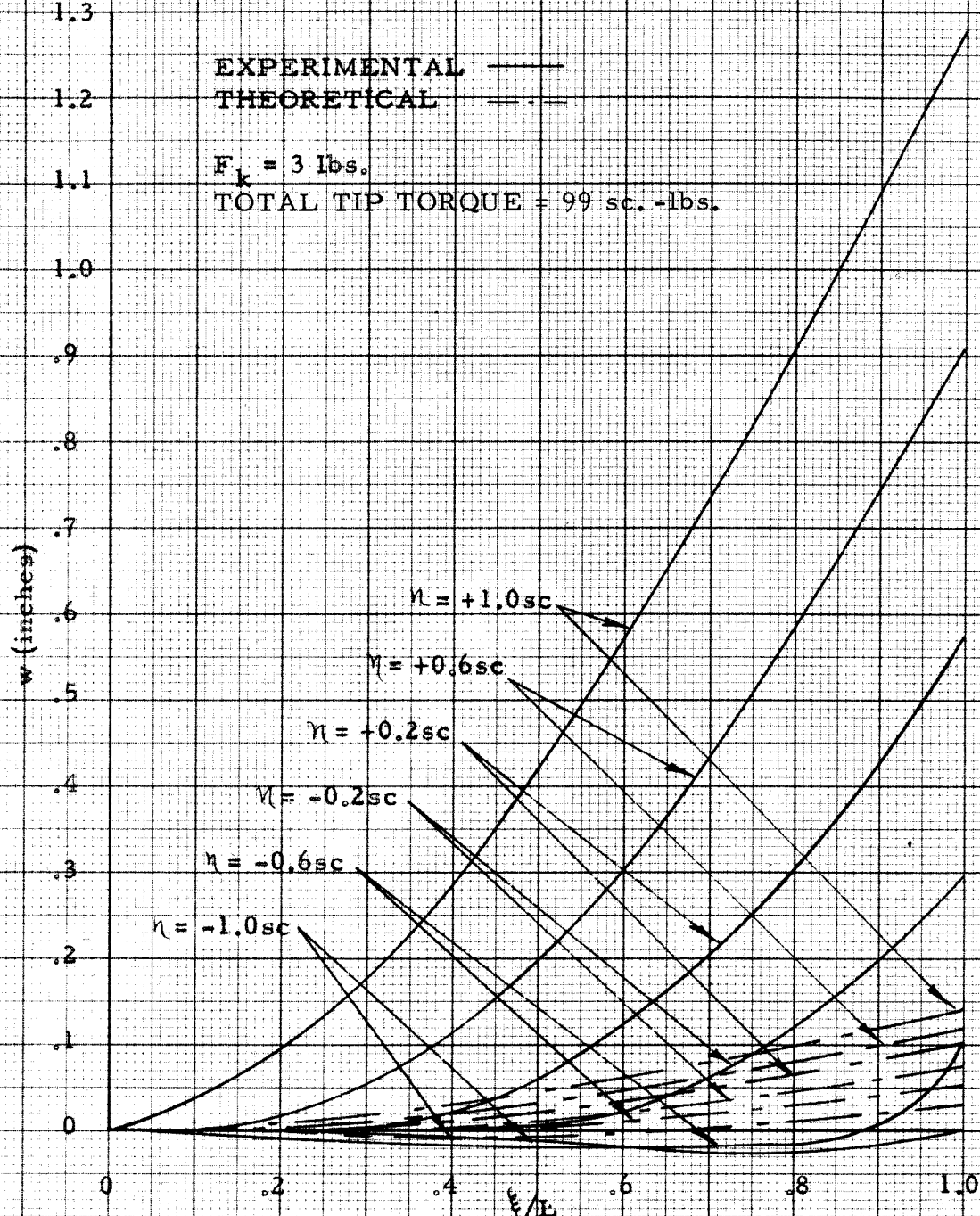

FIGURE 23

CHORDWISE DEFLECTION CURVES FOR
TORSION AT TIP SECTION,
60° SWEEPBACK.

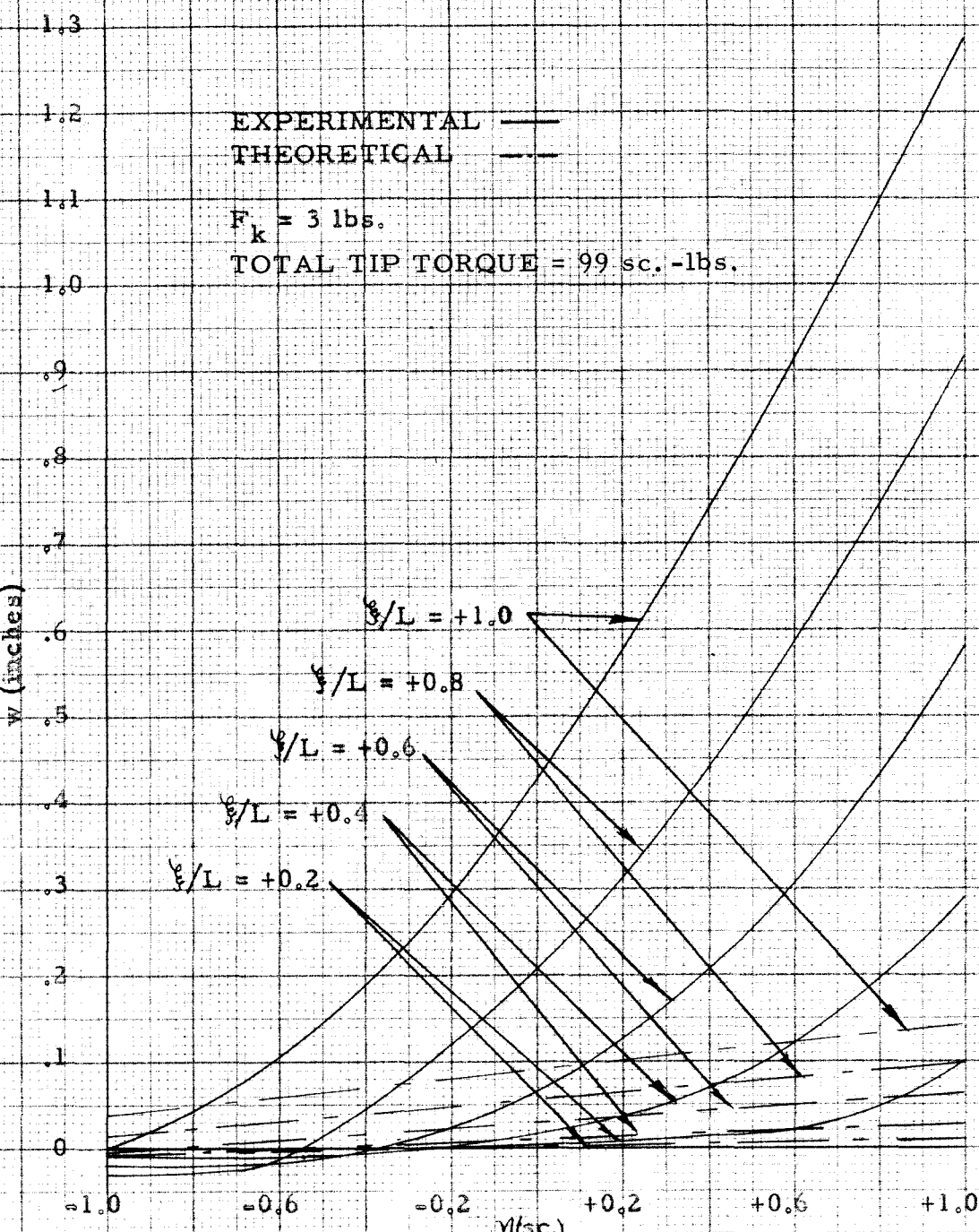

FIGURE 24

Fig. 25

Experimental Set-Up for Finding
Deflections Due to Uniform Surface
Loading at 20° Sweepback.

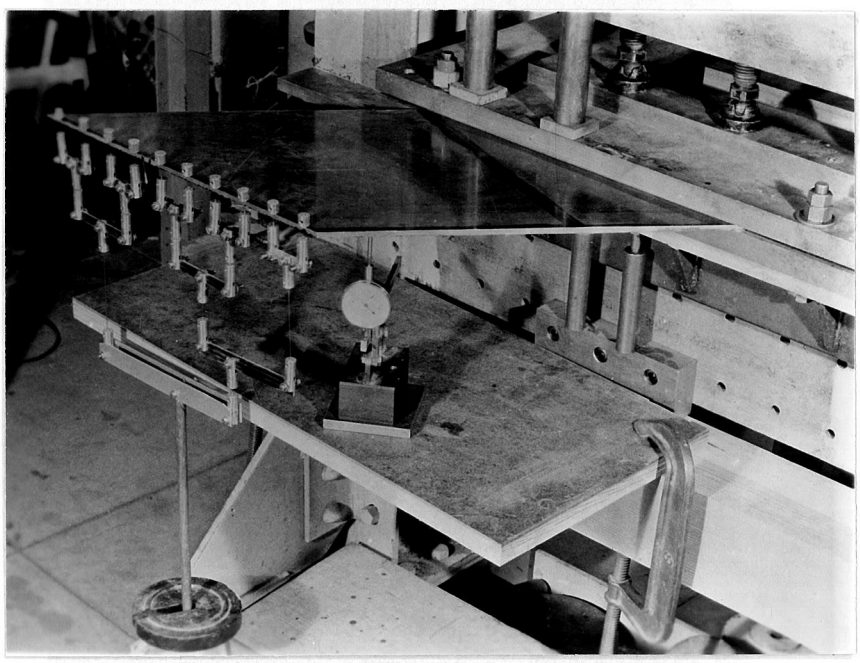

Fig. 26

Experimental Set-Up for Finding
Deflection Due to Uniform Tip Shear
at 40° Sweepback .

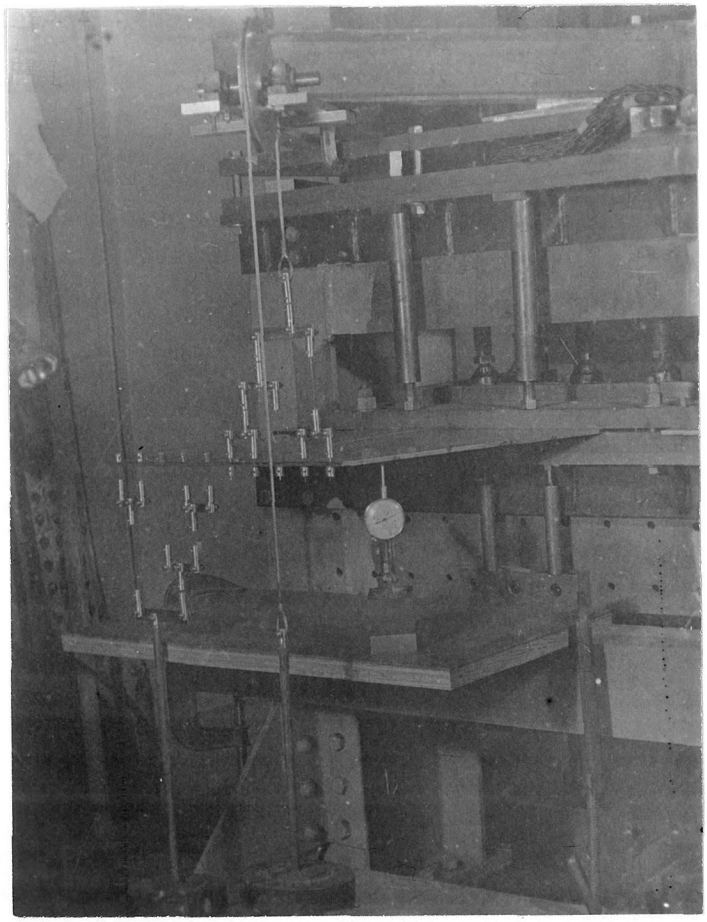

Fig. 27

Experimental Set-Up for Finding
Deflection Due to Torsion at Tip Section
at 20° Sweepback.